Article

Muscle Rev-erb controls time-dependent adaptations to chronic exercise in mice

Jidong Liu [1,2,9], Fang Xiao[3,4,9], Abhinav Choubey[2,9], Udhaya Kumar S [2], Yanxiang Wang[5], Sungguan Hong[2,6], Tingting Yang[2], Husniye Gul Otlu [2,7], Ege Sanem Oturmaz [2], Emanuele Loro[8], Yuxiang Sun [1], Pradip Saha[2], Tejvir S. Khurana[8], Li Chen[1], Xinguo Hou [1] ✉ & Zheng Sun [2,4] ✉

The best time of the day for chronic exercise training and the mechanism underlying the timing effects is unclear. Here, we show that low-intensity, low-volume treadmill training in mice before sleep yields greater benefits than after waking for muscle contractile performance and systemic glucose tolerance. Baseline muscle performance also exhibits diurnal variations, with higher strength but lower endurance before sleep than after waking. Muscle-specific knockout of circadian clock genes *Rev-erbα/β* (Rev-MKO) in male mice eradicates the diurnal variations in both training and baseline conditions without affecting muscle mass, mitochondrial content, food intake, or spontaneous activities. Multi-omics and metabolic measurements reveal that Rev-erb suppresses fatty acid oxidation and promotes carbohydrate metabolism before sleep. Thus, the muscle-autonomous clock, not feeding or locomotor behaviors, dictates diurnal variations of muscle functions and time-dependent adaptations to training, which has broad implications in metabolic disorders and sports medicine as Rev-erb agonists are exercise mimetics or enhancers.

Regular physical exercise is the primary preventive measure and effective medicine for aging-associated deterioration of muscle functions and metabolic disorders[1,2]. As exercise's health benefits gain recognition, there is a growing need to identify the most effective training regimen to maximize benefits while minimizing risk or injury. Numerous studies aim to understand the optimal intensity, volume, or frequency of exercise. While we debate over high-intensity interval training (HIIT) versus steady-state cardio[3], a less explored but equally important question is, what is the best time of the day for chronic exercise training? While some observational human studies suggest a more favorable outcome in glycemic control or cardiovascular risks

for afternoon exercise compared to morning exercise[4–7], experimental human studies have not provided a consensus on this question[8–11]. Some experimental human studies suggest that afternoon or evening training is more effective than morning training in lowering blood glucose or triglycerides levels and increasing muscle power output or fatigue resistance[12,13]. However, some studies suggest that morning training is superior to afternoon training[14,15], while others failed to detect the differences[16,17].

The discrepancy in human studies is probably because of the diverse outcomes, the difficulty in accurately controlling exercise timing, exercise intensity, volume, and measurement timing across

[1]Department of Endocrinology and Metabolism, Qilu Hospital of Shandong University, Jinan, Shandong 250101, China. [2]Department of Medicine, Division of Endocrinology, Diabetes, and Metabolism, Baylor College of Medicine, Houston, TX 77030, USA. [3]Department of Cadres Medical Care and Geriatrics, The Second Hospital, Cheeloo College of Medicine, Shandong University, Jinan, Shandong 250101, China. [4]Department of Molecular and Cellular Biology, Baylor College of Medicine, Houston, TX 77030, USA. [5]Jinan AXZE Medical Test Laboratory, Jinan, Shandong 250101, China. [6]Department of Chemistry, Chung-Ang University, Seoul 06974, Republic of Korea. [7]Vocational School of Health Services, Laboratory Techniques Program, Malatya Turgut Ozal University, Malatya 44900, Türkiye. [8]Department of Physiology, University of Pennsylvania, Philadelphia, PA 19004, USA. [9]These authors contributed equally: Jidong Liu, Fang Xiao, Abhinav Choubey. ✉e-mail: houxinguo@sdu.edu.cn; zheng.sun@bcm.edu

separate studies, and individual variations such as chronotype, baseline physical activity, and exercise capacity across recruited subjects. Animal studies are helpful and offer valuable insights by controlling these confounding variables. The immediate transcriptomic and metabolomic responses to an exercise bout at different times have been profiled in mouse muscles[18-20], though it is unclear how genes or pathways identified from these acute exercise studies would impact the long-term effects of chronic exercise training. Voluntary wheel-running training in mice for 4 weeks at the late or middle active phase is more effective than at the early active phase in reducing body weight gain, although the total training workload and energy expenditure varied among different groups with such a voluntary training regimen[21]. Therefore, the time-dependent effects of chronic exercise training skeletal muscle contractile and metabolic functions and the underlying molecular mechanisms are unclear[9,22-24].

In addition to adaptations to training, there are baseline diurnal variations in muscle contractile and metabolic functions. The baseline muscle contractile performance without training shows a diurnal rhythm, with the peak strength and power activities in humans occurring in the late afternoon[25]. In contrast, the aerobic exercise performance or fatigue resistance is less clear[26,27]. Lipids and carbohydrates fuel physical activity. The flexibility of fuel selection is essential for muscle bioenergetics and exercise performance, which is delicately regulated in response to different physiological and nutritional conditions[28]. Metabolic inflexibility, or failure to adapt to environmental challenges, can lead to insulin resistance and metabolic disorders, such as obesity and type 2 diabetes[29]. Muscles not only passively respond to fuel availability but also proactively anticipate it through their intrinsic circadian clock that is aligned with the sleep/wake cycle, locomotor activity, and food availability[18,30-35]. The circadian clock operates in the central nervous system and peripheral tissues independently and cooperatively. Skeletal muscle harbors one of the most robust peripheral circadian oscillators[36]. To what degree the baseline diurnal variations depend on the clock-directed anticipation vs. response to diet or locomotor activities is unclear.

The molecular machinery of the circadian clock is composed of transcription factors in intertwined feedback loops[37]. The nuclear receptor Rev-erbα/β is a key component of the molecular circadian clock machinery. Global Rev-erbα knockout mice display a drastic reduction in voluntary activity, muscle mitochondrial content, and muscle mass[38,39]. It is unknown whether the muscle phenotype in the global knockout mice is due to loss of Rev-erb function in muscles or other organs[38,40]. Rev-erbα/β are nuclear receptors with ligand-binding domains[41], making them more druggable than common transcription factors[42,43]. Pharmacological activation of Rev-erbα with agonists was shown to increase energy expenditure, reduce fat mass, improve dyslipidemia and hyperglycemia in mice, increase muscle mass, boost muscle mitochondrial oxidative capacity, and enhance exercise performance[39,44,45]. Both Rev-erb agonists and antagonists are shown to ameliorate muscle atrophy[46-49]. As they gain popularity as an exercise mimetic or performance enhancer, Rev-erb agonists are prohibited by the World Anti-Doping Agency[45]. Since these small molecules could have non-specific effects[50], it is unclear whether their diverse impacts rely on Rev-erb or off-target effects. Therefore, the physiological function of muscle Rev-erb remains unknown.

In this work, we address these unanswered questions using muscle-specific Rev-erbα/β knockout mouse lines in combination with differential exercise timing. We show that skeletal muscle-specific knockout of circadian clock genes *Rev-erbα/β* (Rev-MKO) eradicates the diurnal variations in both training and baseline conditions without affecting muscle mass, mitochondrial content, food intake, or spontaneous activities. Thus, the muscle-autonomous circadian clock, not feeding or locomotor behaviors, dictates diurnal variations of muscle functions and time-dependent adaptations to training.

Results

Chronic low-intensity, low-volume treadmill training before sleep is better than upon waking

To address the timing effects of chronic exercise, we subjected adult male C57BL/6 mice to treadmill exercise training. We house mice under the regular 12 h light/12 h dark (LD) condition, with light-on at 7AM (Zeitgeber Time ZT0) and light-off at 7PM (ZT12). The treadmill exercise training occurred either before sleep at ZT23-1 (EX_AM) or upon waking at ZT11-13 (EX_PM) at the speed of 10 m/min without inclination for 1 h per day, 3 days per week, over 5–6 months starting at 2.5 months old (Fig. 1a). We chose these two time-points because they minimize disturbance to sleep while maintaining a 12 h interval. They also resemble human exercise training in the evening and morning, respectively, two popular workout times in gyms for most people. We want to define "morning" and "evening" based on light and the Sun's position to avoid subjective interpretations, as human chronotypes can vary. For mice, evening (PM) is the end of the sleep phase, while morning (AM) is the beginning of the sleep phase. The intensity and volume of this exercise training are low for mice. All mice were able to finish training without struggling. We chose the low-intensity, low-volume training regimen because we want our findings to be potentially generalizable to all individuals, including those with limited exercise capacities due to aging or other conditions. Another reason for choosing the low-intensity, low-volume exercise training regimen is that we want to expose the differences between AM and PM exercises rather than maximize the effects of exercise over the 'rest' control. We did not use the running wheel exercise because it is difficult to control exercise intensity, volume, or timing accurately with voluntary running wheels. Mice were group-housed with ad libitum access to a chow diet throughout the experiment.

Compared to the EX_PM group, the EX_AM group has a slower rate of body weight gain and body fat gain without affecting lean mass or average daily food intake (Fig. 1b–d). The lack of significant changes between the EX_PM group and the rest control is not surprising, considering the low intensity and low volume of the training regimen. We performed a series of exercise performance tests at least 24 h after the last training session to avoid the acute effects of training. We tested at both ZT23-1 and ZT11-13 to address the adaptive alignment of peak exercise performance with training time[15,51,52]. For muscle strength, we performed the grip strength test with the Bioseb meter following the manufacturer's instructions. We made great efforts to manage measurement variations by averaging only the highest readings from multiple measurements, allowing mice to rest for at least 5 min between measurement sessions, and using a large sample size. The EX_AM group showed higher strength than EX_PM and rest control at both ZT23-1 and ZT11-13 (Fig. 1e). We also performed the wire hang test as described[53]. EX_AM showed a more prominent improvement over the Rest control than EX_PM (Fig. 1f). For the graded exercise test, mice were motivated by electric shocks to run a treadmill at a low-speed profile (Fig. 1g). Shocks received for each mouse were recorded automatically, and 50 cumulative shocks defined exhaustion as described previously[54]. EX_AM showed a more pronounced improvement than EX_PM in endurance (Fig. 1h) without pronounced changes in the weight of extensor digitorum longus (EDL), tibialis anterior (TA), and soleus muscles. Marker genes of myofiber types did not show significant changes between EX_AM and EX_PM either (Supplementary Fig. S1). We also performed glucose tolerance tests (GTT) at different ZTs and found that EX_AM significantly improved glucose tolerance over
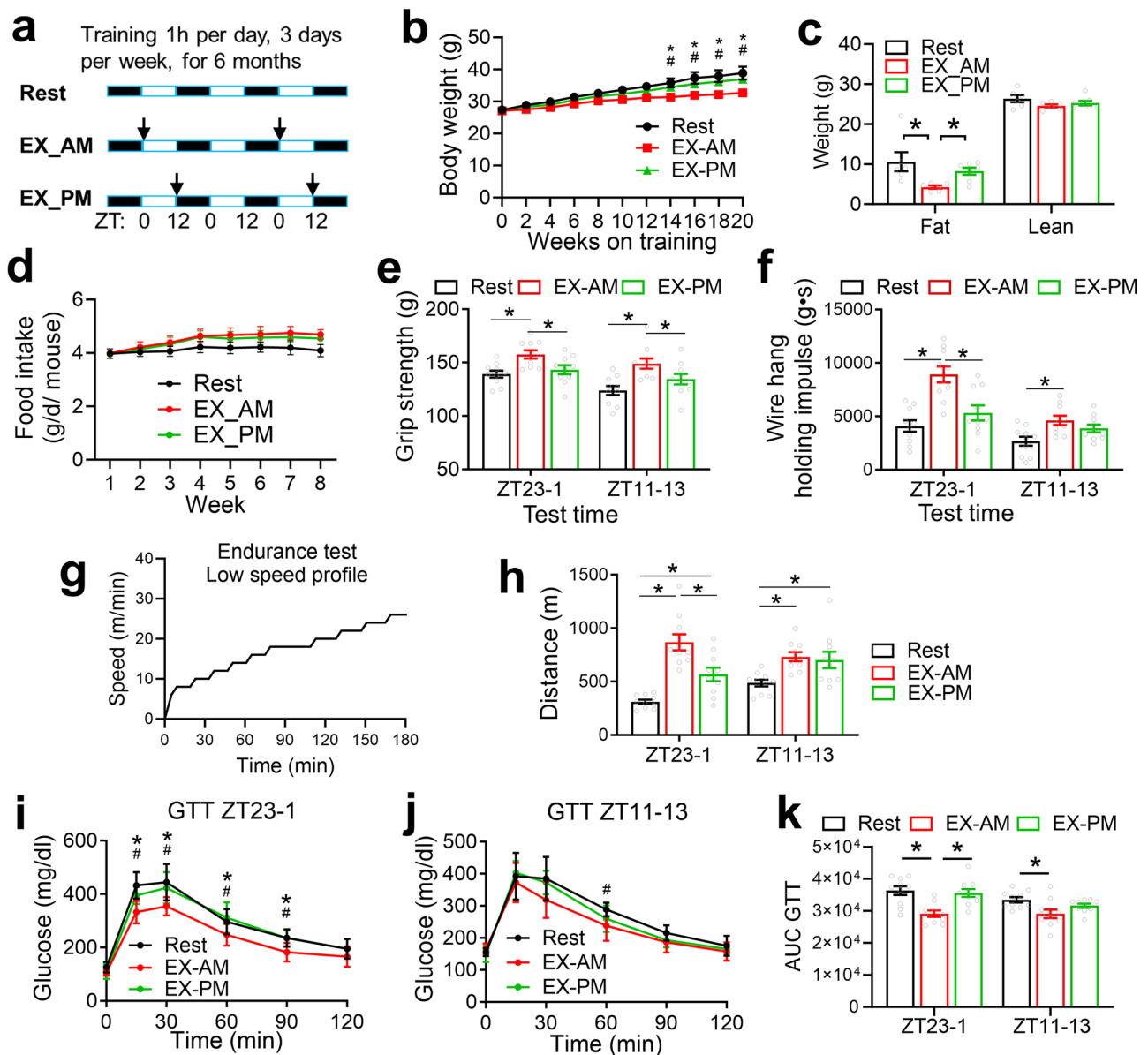
Fig. 1 | Low-intensity exercise before sleep is better than after waking for weight control, contractile performance, and glucose tolerance. a Treadmill training scheme. **b** Body weight ($n = 10$ mice/group), *$p = 0.0067$, 0.0161, 0.0191, and 0.0147 for EX_AM vs. EX_PM; #$p = 0.0316$, 0.0363, 0.0358, and 0.0360 for EX_AM vs. Rest, with 2-way repeated-measure ANOVA and Tukey test. **c** Magnetic resonance imaging (MRI) analysis of body composition at 6 months of age ($n = 6$ mice for Rest, $n = 7$ mice for EX_AM or EX_PM). *$p = 0.0013$ (Rest vs. EX_AM) and 0.0316 (EX_AM vs. EX_PM) by 2-way ANOVA and Holm-Sidak test. **d** Average daily food intake at 6 months old ($n = 10$ mice). **e** Forelimb grip strength at 7 months old ($n = 10$). *$p = 0.0095$ (EX-AM vs. Rest at ZT23-1), 0.0392 (EX-AM vs. EX-PM at ZT23-1), 0.0003 (EX-AM vs. Rest at ZT11-13), and 0.036 (EX-AM vs. EX-PM at ZT11-13) by 2-way ANOVA and Holm-Sidak test. **f** Wire hang tests at 7 months old ($n = 10$ mice). *$p = 0.0001$ (EX-AM vs. Rest at ZT23-1), 0.0001 (EX-AM vs. EX-PM at ZT23-1), and

0.046 (EX-AM vs. Rest at ZT11-13) by 2-way ANOVA and Holm-Sidak test. **g** Treadmill speed profile. **h** Distance traveled before receiving 50 shocks at 7 months old ($n = 10$ mice). *$p = 0.0001$ (EX-AM vs. Rest at ZT23-1), 0.002 (EX-PM vs. Rest at ZT23-1), 0.0007 (EX-AM vs. EX-PM at ZT23-1), 0.0085 (EX-AM vs. Rest at ZT11-13), and 0.0165 (EX-PM vs. Rest at ZT11-13) by 2-way ANOVA and Holm-Sidak test. **i, j** GTT at 8 months old ($n = 10$ mice). Data are mean ± SD. *$p = 0.0035$, 0.013, 0.0325, and 0.0068 for EX-AM vs. EX_PM; #$p = 0.0004$, 0.0074, 0.0495, and 0.0068 at ZT23-1 or 0.0256 at ZT11-13 for EX-AM vs. Rest with 2-way repeated-measure ANOVA and Holm-Sidak test. **k** Area under the curve (AUC) for the GTT tests. *$p = 0.0001$ (EX-AM vs. Rest at ZT23-1), 0.0004 (EX-AM vs. EX-PM at ZT23-1), and 0.0184 (EX-AM vs. Rest at ZT11-13) by 2-way ANOVA and Tukey test. Data are mean ± SEM unless otherwise specified.

the rest control regardless of what time we tested, while EX_PM did not show significant improvement, probably due to the low volume of exercise (Fig. 1i–k). The improvement in the EX_AM group are impressive for healthy wild-type mice fed on a normal chow diet without baseline metabolic disruptions. The improvement is more obvious when tested before sleep than after waking, probably because the non-exercise baseline has better glucose tolerance after waking compared to before sleep. Considering that mice are nocturnal while humans are diurnal, these data are consistent with

human studies that show a better glucose-lowering effect of exercise in the evening compared to exercise in the morning[12,13]. We also observed better performance when the testing time was aligned with the training time, compared to misaligned testing/training pairs, in line with previous human studies[15,51,52]. However, the difference in testing time does not obliterate the time-dependent effects of training. In summary, training before sleep has more benefits overall than after waking in terms of improving muscle contractile functions and systemic glucose metabolism.
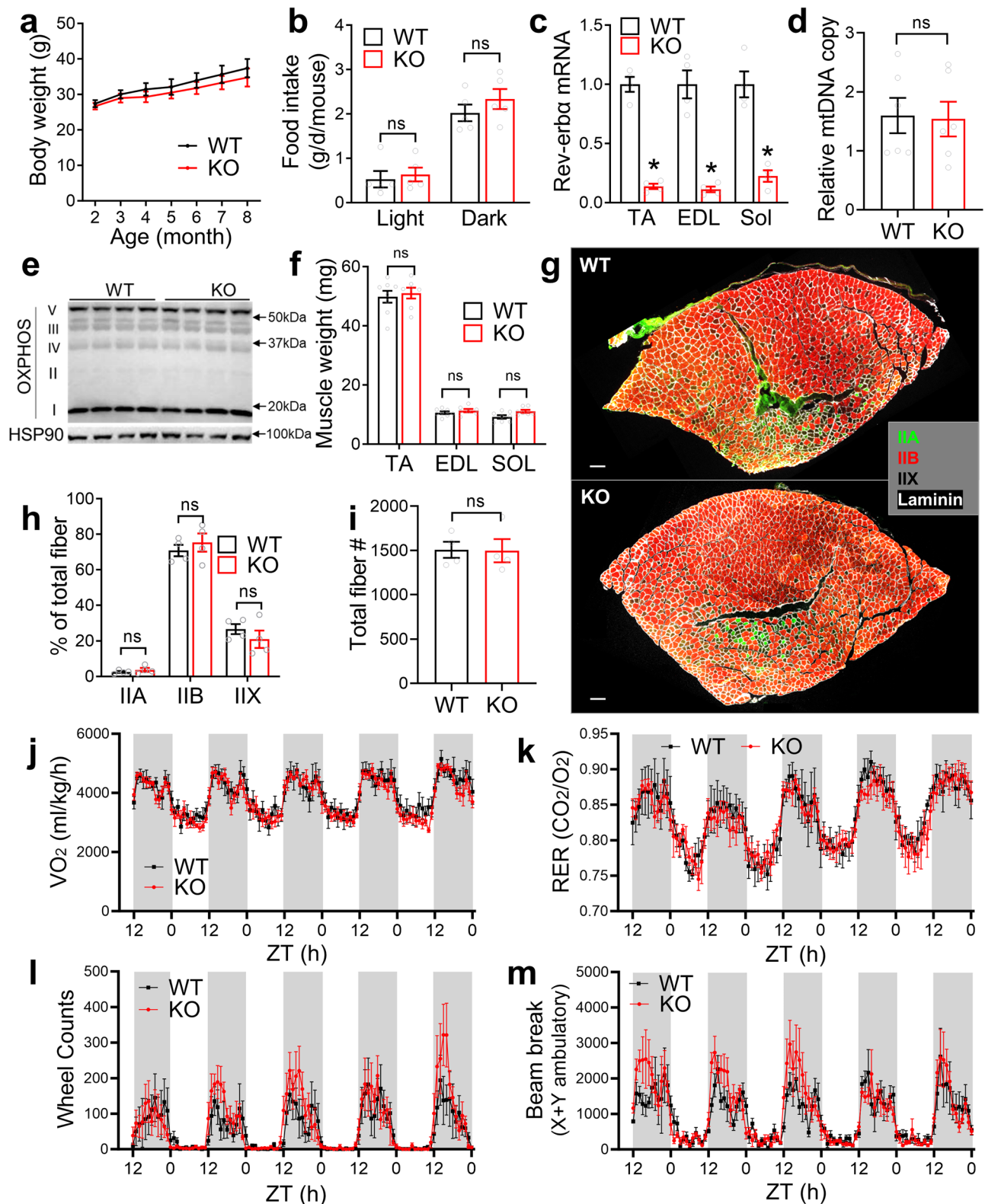
Muscle Rev-erb does not affect baseline mitochondrial content, muscle mass, fiber type composition, locomotor activities, or energy expenditure

To address the role of muscle circadian clock in time-dependent training effects, we generated skeletal muscle-specific Rev-erbα/β double knockout (Rev-MKO or simply KO) by crossbreeding mice bearing *Rev-erbα*[loxP] (MGI ID 5426700) and *Rev-erbβ*[loxP] (MGI ID 5426699) alleles[55] with the MLC-Cre line (MGI ID 1931135)[56]. The *Rev-erbα*[loxP] allele gives rise to a truncated Rev-erbα protein without the DNA-binding domain (DBD) after Cre recombination. Littermate mice bearing *Rev-erbα*[loxP]/*Rev-erbβ*[loxP] alleles without Cre or the Cre allele without Rev-erbα/β[loxP] were used as the wild-type (WT) control. KO mice were born at the Mendelian ratio and showed normal body size and activity. We first performed a series of phenotype characterizations at the baseline without training. The Rev-MKO mice show normal body weight and food intake (Fig. 2a, b) and efficient deletion of Rev-

Fig. 2 | Rev-MKO mice show normal baseline mitochondrial content, muscle mass, fiber type, locomotor activities, and energy expenditure. a Body weight. n = 8 mice for WT (4 Rev-erb[floxed] and 4 MLC-Cre), n = 7 mice for KO. **b** Average food intake at 6 months of age (n = 5 mice per group). For WT, 3 Rev-erb[floxed] and 2 MLC-Cre. Analyzed by 2-sided student t-test. **c** RT-qPCR analysis of the tibialis anterior (TA), extensor digitorum longus (EDL), and soleus (Sol) muscle from 8 month-old male mice harvested at ZT6 using primer pairs that span the floxed exons in Rev-erbα (n = 4 mice per group). For WT, 2 Rev-erb[floxed] and 2 MLC-Cre. *p < 0.0001 for WT vs. KO by 2-sided unpaired student t-test. **d** Relative mitochondrial copy number by qPCR analysis in EDL muscles at 6 months of age (n = 6 mice per group). For WT, 3 Rev-erb[floxed] and 3 MLC-Cre. Analyzed by 2-sided student t-test. **e** Western blot analysis of mitochondrial OXPHOS protein complexes in quadriceps muscle at

6 months of age (n = 4 mice per group, repeated 2 times). For WT, 2 Rev-erb[floxed] and 2 MLC-Cre. **f** Muscle weight at 6 months of age (n = 8 mice for WT and n = 7 mice for KO). For WT, 4 Rev-erb[floxed] and 4 MLC-Cre. Analyzed by 2-sided student t-test. (**g**) Representative immunofluorescence staining (from 3 replicates) of cross-sections of tibialis anterior (TA) muscles at 6 months of age. Scale bar = 200 μm. **h, i** Quantification of the muscle fiber composition and total fiber number at 6 months of age (n = 4 mice per group). For WT, 2 Rev-erb[floxed] and 2 MLC-Cre. Analyzed by 2-sided student t-test. **j−m** Oxygen consumption rate (VO₂), respiratory exchange ratio (RER), voluntary wheel-running counts, and beam breaks as measured by the Oxymax/CLAMS-HC system at 6 months of age (n = 5 mice per group). For WT, 3 Rev-erb[floxed] and 2 MLC-Cre. ns, not significant. Data are mean ± SEM.

erbα/β in limb muscles examined at ZT6, including tibialis anterior (TA), extensor digitorum longus (EDL), and soleus (Sol) muscles (Fig. 2c). Rev-erb-depleted muscles have the normal mitochondrial DNA copy number (Fig. 2d), oxidative phosphorylation (OXPHOS) protein content (Fig. 2e), muscle mass (Fig. 2f), muscle fiber type composition and fiber numbers (Fig. 2g–i). Rev-MKO mice also have normal rhythmicity of oxygen consumption (Fig. 2j), respiratory exchange ratio (RER) (Fig. 2k), voluntary wheel-running activity (Fig. 2l), and spontaneous beam-breaking locomotor activity (Fig. 2m) under regular LD conditions. Thus, muscle-specific deletion of Rev-erb does not cause a fundamental disruption of muscle function or energy homeostasis at the baseline without exercise training.

The time-dependent training effects require muscular Rev-erb

To address the role of muscle Rev-erb in chronic exercise training-induced adaptations, we subjected WT and Rev-MKO mice to chronic training at either AM or PM as described starting from 2.5 months old (Fig. 1a). Consistent with the previous mouse cohort, the WT EX_AM and WT EX_PM groups showed significant differences in body weight (Fig. 3a), grip strength (Fig. 3b), wire hang performance (Fig. 3c), treadmill exercise test at a low speed profile (Fig. 3d), and glucose tolerance (Fig. 3e, f). Remarkably, all these EX_AM vs. EX_PM differences were abolished in Rev-MKO mice (Fig. 3a–f). The results were reproduced in another mouse cohort with non-training baseline controls (Supplementary Fig. S2a–g). We then used the non-invasive protocol[57–59] to measure hindlimb isometric torque in vivo for Plantor flexor contraction at tetanic (100 Hz stimulation) and sub-tetanic (40 Hz stimulation) for fatigue resistance profiling. EX_AM showed a more pronounced benefit than EX-PM in WT groups, a difference abolished in Rev-MKO groups (Supplementary Fig. S2h–j). We also measured the dorsiflexion contractions at different times of the day. The WT EX_AM group showed consistently greater improvement than the WT EX_PM group in tetanic force generation at 100 Hz stimulation (Fig. 3g, h) and sub-tetanic fatigue resistance at 40 Hz stimulation (Fig. 3i–l), regardless of the test time. Again, the differences between EX_AM and EX_PM were completely abolished in the Rev-MKO mice (Fig. 3g–l). Subtracting the non-exercise baseline from the trained groups of the same genotype also reached the same conclusion (Supplementary Fig. S3). In summary, these results demonstrate that muscular Rev-erb is required for the time-dependent effects of chronic training.

Muscle Rev-erb regulates time-dependent metabolic adaptations to chronic training

Since muscle Rev-erb does not affect baseline energy homeostasis, how does it mediate the AM vs. PM differences in training-induced fat mass loss? We investigated how training at AM vs. PM affects energy balance differently in the WT and KO lines. To avoid confounding effects of body weight, we performed indirect calorimetry analysis and body temperature measurements after exercise training for only 2 months before body weight differences became significant (Fig. 4a–n). All groups have similar total food intake and body weight

(Fig. 4a, b). Compared to WT EX_PM, WT EX_AM showed a moderately but significantly higher daily O₂ consumption (Fig. 4c, e). The differences are most pronounced during the wake cycle immediately after the training day (Fig. 4e). In line with the oxygen consumption, the WT EX_AM group showed higher voluntary wheel-running (Fig. 4g) and beam-breaking activities than EX_PM (Fig. 4i, k). Beam activity in the dark cycle following the exercise day is quantified in Fig. 4k. Consistent with the higher energy expenditure and spontaneous activity, the WT EX_AM group showed higher body temperature in the wake cycle than the WT EX_PM group (Fig. 4l, m). These data suggest that PM training suppressed spontaneous locomotor activities more than AM training in WT mice, which might contribute to the overall higher energy expenditure, leading to lower body fat in the WT EX_AM group than in the WT EX_PM group (Fig. 1). Interestingly, the time-dependent training effects on energy expenditure, spontaneous locomotor activities, and body temperature were completely abolished in Rev-MKO mice after the same exercise training sessions as in WT mice (Fig. 4d, f, h, j, k, l, n). Plotting the results with the non-training baseline values or subtracting the baseline from the training groups reached the same conclusion (Supplementary Fig. S4). In summary, these results suggest that muscle Rev-erb is required for training-dependent suppression of spontaneous locomotor activity. Therefore, we speculate that muscle Rev-erb could regulate muscle fatigue at the baseline without training.

Muscular Rev-erb regulates muscle fatigue resistance and strength

We characterized the baseline muscle performance in WT and Rev-MKO mice. WT mice showed higher strength before sleep (ZT23-1) than upon waking (ZT11-13) (Fig. 5a, b), which is in line with human studies that show peak strength in late afternoon[25]. Of note, these are the baseline variations without exercise training. The data reflects the natural variation across these time points, not the effects of training. Such baseline diurnal variations were abolished in the KO mice with constantly low strength (Fig. 5a, b). In contrast to the strength, the treadmill exercise test with a low-speed profile showed higher endurance before sleep than upon waking in WT mice (Fig. 5c). Interestingly, KO mice showed higher endurance than WT before sleep (Fig. 5c), which abolished the diurnal variation in endurance. Similar results were observed in female mice (Fig. 5d, e). The in vivo muscle physiology analysis confirmed reduced muscle strength (Fig. 5f) but increased muscle fatigue resistance in KO than WT mice (Fig. 5g, h), especially before sleep. This in vivo result was further confirmed with an ex vivo muscle physiology analysis showing reduced strength (Fig. 5i–k) but enhanced fatigue resistance (Fig. 5l) and force recovery after exhaustion (Fig. 5m) in isolated EDL muscles from KO than WT mice in a procedure as previously described[54,60]. The specific force showed a less significant difference (p = 0.09) between KO and WT (Fig. 5k) because the KO mice had a slightly insignificant lower cross-section area (CSA). We speculate that baseline diurnal variations in endurance and fatigue resistance contribute to time-dependent, training-induced suppression of locomotor activities in WT mice (Fig. 4k). Of note, the higher exercise endurance in KO mice was only
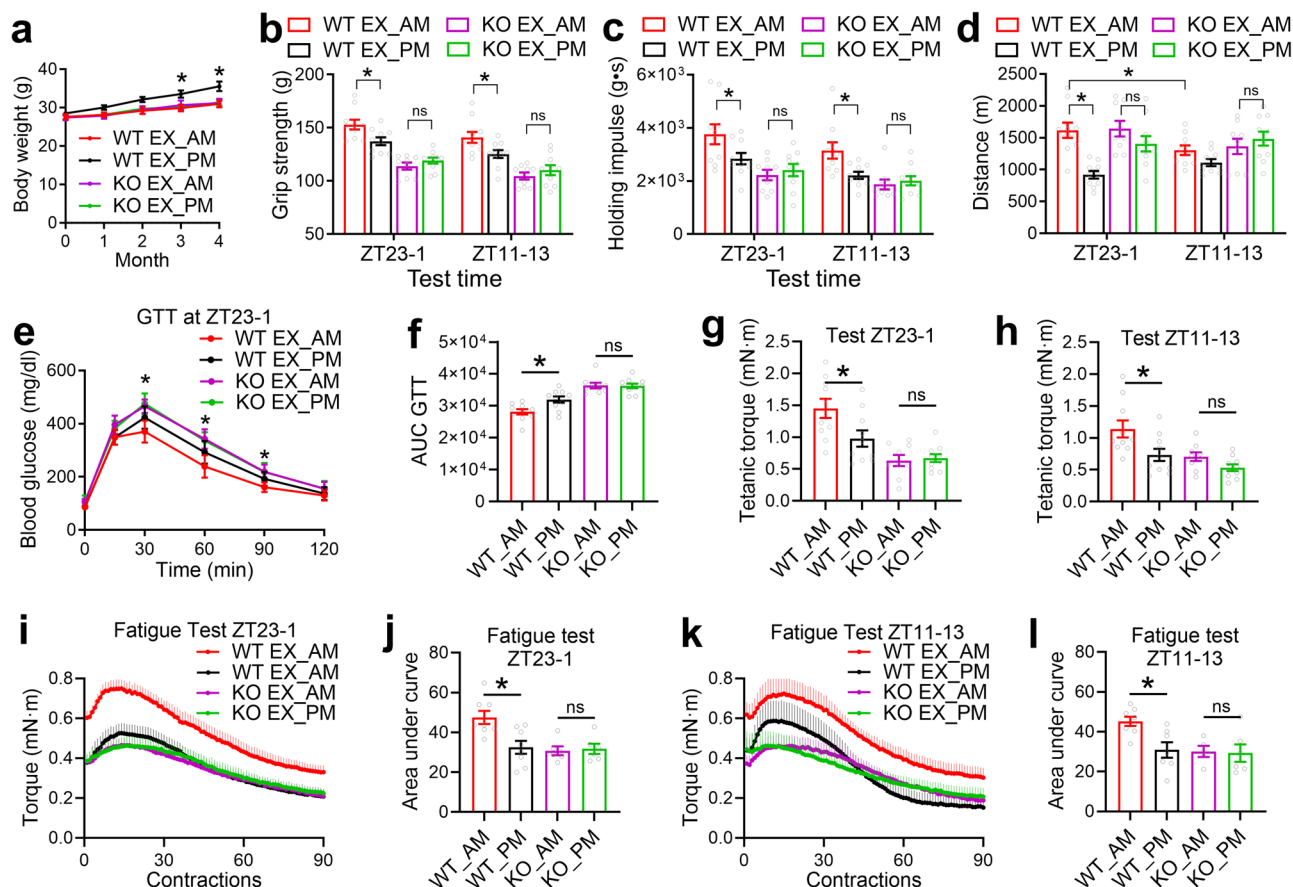
Fig. 3 | Muscle Rev-erb is required for the timing effects of exercise training on weight control, contractile performance, and glucose tolerance. a Body weight ($n = 9$ mice for KO EX_AM, $n = 10$ mice for the other groups). *$p = 0.0473$ and 0.042 for WT EX_AM vs. WT EX_PM with 2-way repeated-measure ANOVA and Tukey test. WT, Rev-erb[floxed] mice. **b**, **c** Forelimb grip strength test and wire hang test at 6 months old ($n = 9$ mice for KO EX_AM, $n = 10$ mice for the other groups). *$p = 0.0318$ (ZT23-1) and 0.0332 (ZT11-13) for grip strength, 0.0409 (ZT23-1) and 0.0346 (ZT11-13) for wire hang, by 2-way ANOVA and Tukey test. **d** Treadmill distance at 7 months old ($n = 9$ mice for KO EX_AM, $n = 10$ mice for the other groups). *$p = 0.0001$ (EX-AM vs. EX-PM at ZT23-1) and 0.0297 (ZT23-1 vs. ZT11-13 for WT EX_AM) by 2-way ANOVA and Tukey test. **e** GTT at ZT 23-1 at 8 months old ($n = 9$

mice for KO EX_AM, $n = 10$ mice for the other groups). Data are mean ± SD. *$p = 0.0414$, 0.0486 and 0.0236 for WT_EX_AM vs. WT_EX_PM with 2-way repeated-measure ANOVA and Holm-Sidak test. **f** Area under the curve (AUC) in GTT. *$p = 0.0149$ with 1-way ANOVA and Tukey test. **g**, **h** Dorsi flexor tetanic torque at 9 months old ($n = 9$ mice for KO EX_AM, $n = 10$ mice for the other groups). *$p = 0.0255$ (ZT23-1) and 0.0193 (ZT11-13) by 1-way ANOVA and Tukey test. **i–l** Fatigue analysis at 9 months old at ZT23-1 ($n = 8$ mice for WT, $n = 6$ mice for KO) or ZT11-13 ($n = 8$ mice for WT EX_AM, $n = 7$ mice for WT EX_PM, $n = 5$ for KO EX_AM, $n = 6$ mice or KO EX_PM). *$p = 0.0053$ (ZT23-1) and 0.0202 (ZT11-13) by 1-way ANOVA and Tukey test. Data are mean ± SEM unless otherwise specified. ns, not significant.

observed with the low-speed profile (Fig. 5n–p) but not with a high-intensity speed profile (Fig. 5q–s), suggesting that it is attributable to bioenergetics adaptations rather than muscular structural alterations.

Multi-omics characterization of muscle Rev-erb functions

To dissect the molecular mechanism underlying how Rev-erb regulates muscle contraction and fatigue resistance, we performed RNA-seq in the TA muscles of WT and KO mice at ZT10 and ZT22 because these time points correspond to the peak and trough Rev-erbα protein levels in muscles[54] and immediately precede the exercise training and testing timepoints in our prior tests (ZT11-13 and ZT23-1, respectively). More differentially expressed genes (DEGs) between KO and WT were found in ZT22 compared to ZT10 (Fig. 6a), in keeping with the more drastic phenotypic differences at ZT23-1 in KO vs. WT mice (Fig. 5). KEGG pathway analysis revealed that genes involved in amino acid catabolism and lipid oxidation are upregulated in KO vs. WT muscles, while glycolytic genes are downregulated (Fig. 6b–d). The apparent upregulation of Rev-erbα itself in KO vs. WT is due to abolishment of the self-negative feedback as Rev-erbα represses its own transcription. Genes involved in contraction, ion transport, adhesion, sarcomere,

and insulin signaling were also downregulated in KO vs. WT muscles, especially at ZT22 (Fig. 6e).

We compared the Rev-erb-dependent transcriptomic changes to those regulated by Bmal1[61], a core clock gene and direct transcriptional activator of Rev-erb. Out of 190 Bmal1-dependent DEGs (muscle-specific knockout of Bmal1 or Bmal1-MKO vs. WT at ZT20), 116 were shared with Rev-erb (Rev-MKO vs WT at ZT22) (Supplementary Fig. S5a). For ZT8-10, out of 116 Bmal1-dependent DEGs at ZT8, 65 were shared with Rev-erb at ZT10 (Fig. S5b). The overlapping DEGs (pooled from both time points) were enriched in circadian rhythm, ion transport, and organic acid transport (Fig. S5c). While Rev-erb-unique DEGs were enriched in lipid metabolism and cell adhesion (Fig. S5d), Bmal1-unique DEGs were enriched in carbohydrate transport, muscle development, and muscle differentiation (Fig. S5e). Although there are inherent limitations in such comparisons, as RNA-seq generally detects more DEGs than microarray and the ZTs for sample collection are not perfectly aligned between studies, the comparison suggests that while Bmal1 and Rev-erb share overlapping functions in muscles, they also maintain distinct roles unique to each.

Chromatin immunoprecipitation of Rev-erbα (ChIP-seq) in muscles revealed that genome-wide binding of Rev-erbα at ZT10 were
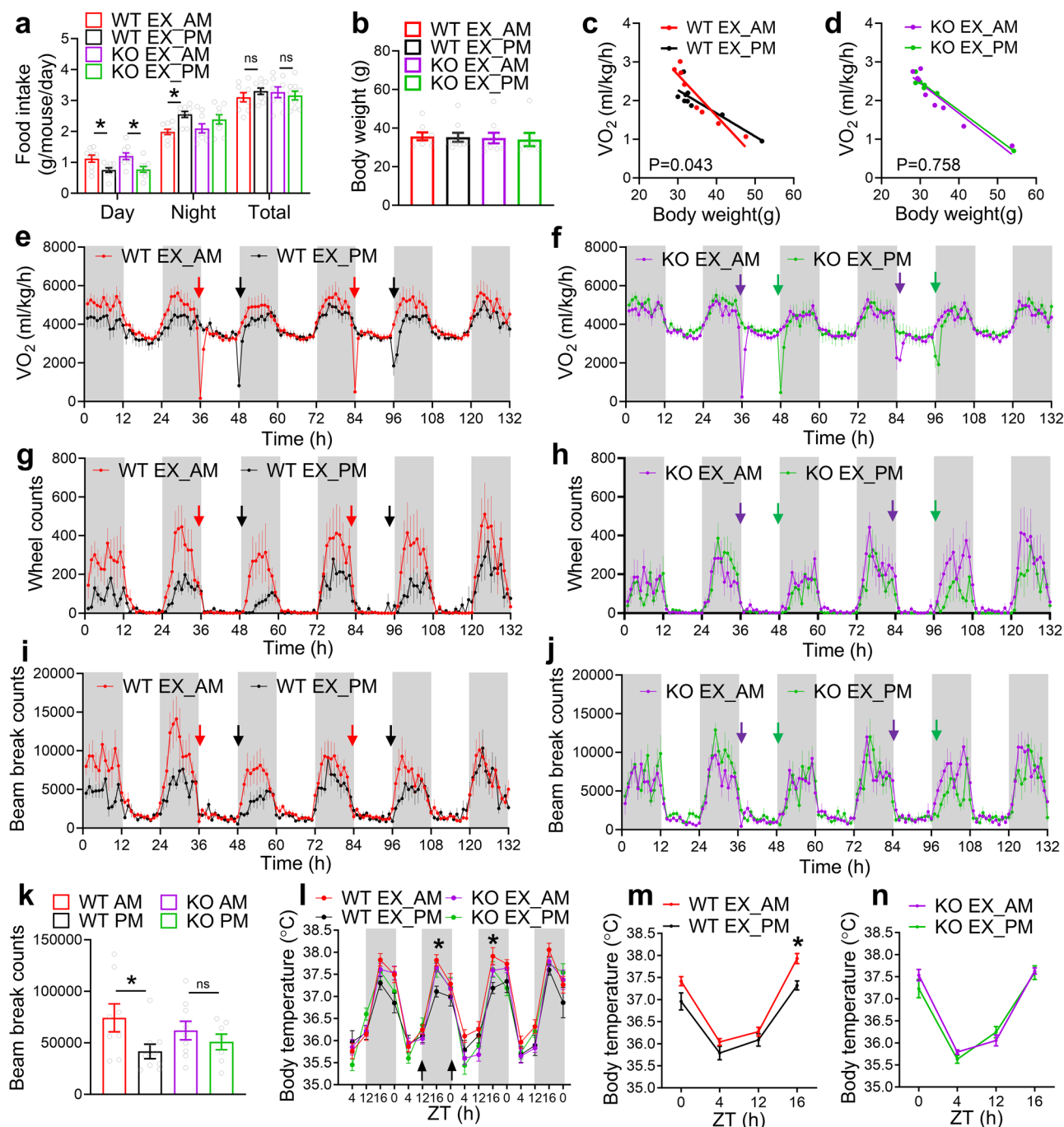
Fig. 4 | Muscle Rev-erb is required for the time-dependent effects of chronic exercise on energy balance and locomotor activity. a Average daily food intake ($n = 9$ mice/group). WT are Rev-erb[floxed] mice. *$p = 0.0452$, 0.0208, and 0.0183 by 1-way ANOVA and Holm-Sidak test. b Body weight at 4.5 months old ($n = 8$ mice for WT EX_AM, $n = 9$ mice for WT EX_PM, $n = 9$ mice for KO EX_AM, $n = 7$ mice for KO EX_PM). c, d Linear regression analysis (2-sided) of average daily oxygen consumption vs. body weight at 4.5 months old ($n = 8$ mice for WT EX_AM, $n = 9$ mice for WT EX_PM, $n = 9$ mice for KO EX_AM, $n = 7$ mice for KO EX_PM). e–j Oxygen consumption, voluntary wheel-running activity, and spontaneous beam-breaking activity as measured by the Oxymax/CLAMS-HC system at 4.5 months old ($n = 8$

mice for WT EX_AM, $n = 9$ mice for WT EX_PM, $n = 9$ mice for KO EX_AM, $n = 7$ mice for KO EX_PM). Arrows indicate a temporary disruption when mice were taken out for treadmill exercise sessions. k Average daily beam break counts at 4.5 months of age ($n = 8$ mice for WT EX_AM, $n = 9$ mice for WT EX_PM, $n = 9$ mice for KO EX_AM, $n = 7$ mice for KO EX_PM). *$p = 0.0431$ by 1-way ANOVA and Sidak test. l–n Rectal temperature across different days or average temperature from multiple days at 4.5 months old ($n = 11$ mice for WT EX_AM, $n = 10$ mice for the other groups). Arrows indicate treadmill sessions. *$p = 0.0034$ and 0.0301 (WT_EX_AM vs. WT_EX_PM for panel l) and 0.0034 (WT_EX_AM vs. WT_EX_PM for panel m) by 2-way ANOVA and Tukey test. All data are mean ± SEM. ns, not significant.

enriched in the promoter regions (Fig. 6f). The motif shared by Rev-erb and RAR-related orphan receptor (ROR)[62–64], known as ROR response elements (RORE), is among the top motifs enriched in Rev-erbα ZT10 peaks (Fig. 6g). Rev-erbα has far more binding sites (Fig. 6h) and higher binding strength (Fig. 6i) at ZT10 than at ZT22. These results suggest a

time delay between the peak Rev-erb expression and the maximum downstream transcriptomic effect, which is in line with the notion that Rev-erb anticipates the dark cycle. Indeed, strong Rev-ebα peaks were found at ZT10 but not at ZT22 in the near DEGs involved in amino acid and lipid metabolism (Fig. 6j, k). By comparison, Rev-erbα peaks were
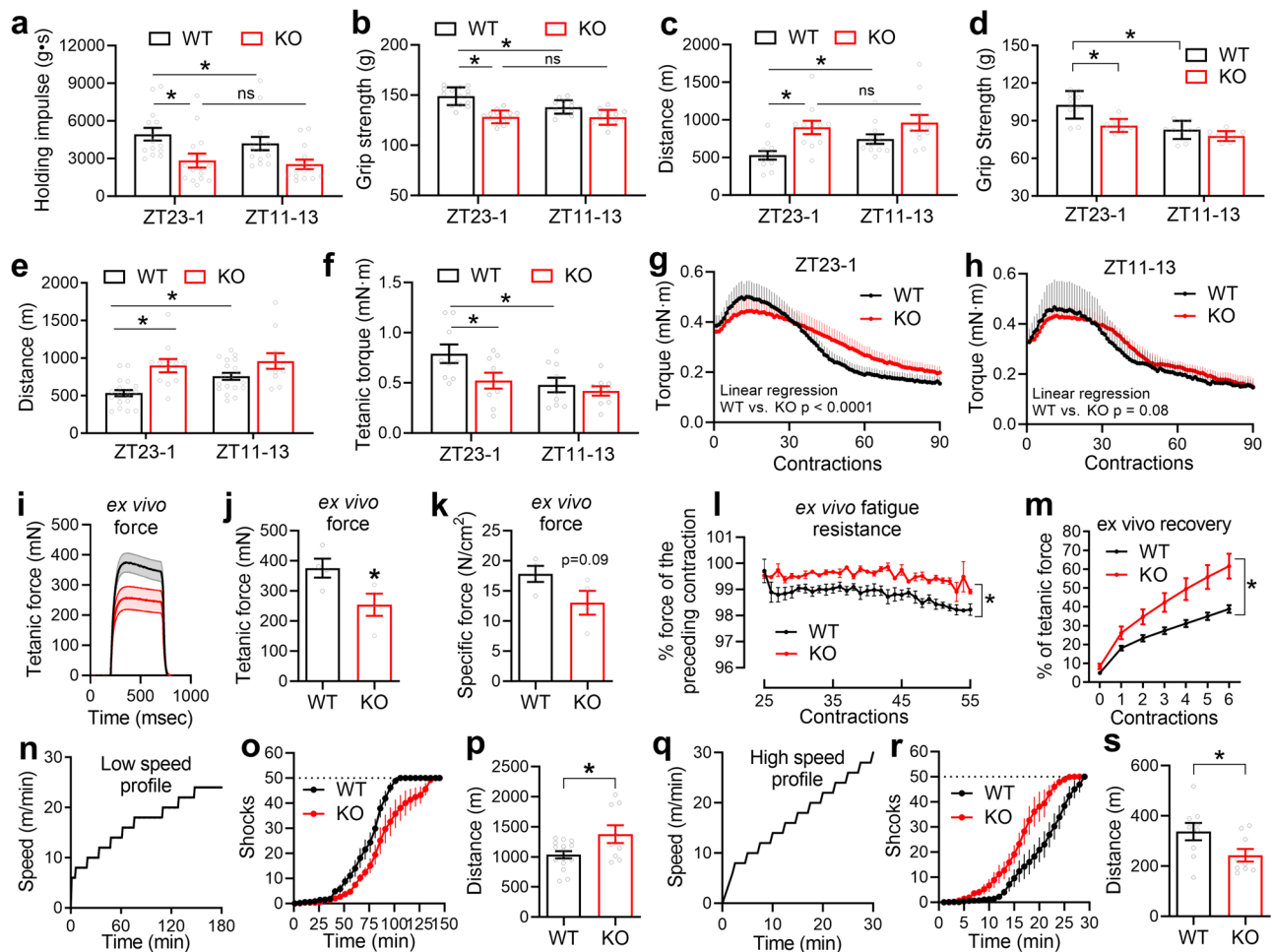
Fig. 5 | Muscle Rev-erb regulates the baseline diurnal rhythm of muscle strength and endurance. a Wire hang in males at 3 months old. *$p = 0.0085$ (WT vs. KO at ZT23-1) and 0.0255 (ZT23-1 vs. ZT11-13 for WT). **b** Forelimb grip strength in males at 3 months old. *$p = 0.001$ (WT vs. KO at ZT23-1) and 0.0001 (ZT23-1 vs. ZT11-13 for WT). Data are mean ± SD. **c** Treadmill test with the low-speed profile in males at 4 months old. *$p = 0.0047$ (WT vs. KO at ZT23-1) and 0.0424 (ZT23-1 vs. ZT11-13 for WT). (a-c) $n = 14$ mice/group. WT are 9 Rev-erb^{floxed} and 5 MLC-Cre. **d** Forelimb grip strength in females at 4 months old ($n = 10$ mice/group). WT are Rev-erb^{floxed} mice. Data are mean ± SD. *$p = 0.0001$ (WT vs. KO at ZT23-1) and 0.0001 (ZT23-1 vs. ZT11-13 for WT). **e** Treadmill test in females with the low-speed profile at 3 months old ($n = 19$ WT, 11 KO). WT are Rev-erb^{floxed} mice. *$p = 0.0005$ (WT vs. KO at ZT23-1)

and 0.0034 (ZT23-1 vs. ZT11-13 for WT). **f** Dorsi flexor tetanic torque in vivo in males at 9 months old ($n = 9$). WT are Rev-erb^{floxed} mice. *$p = 0.0323$ (WT vs. KO at ZT23-1) and 0.0492 (ZT23-1 vs. ZT11-13 for WT). **a**–**f** were determined by 2-way ANOVA and Holm-Sidak test. **g**, **h** Dorsi flexor fatigue resistance in vivo in males at 9 months old at ZT23-1 ($n = 8$ WT, 10 KO) or ZT11-13 ($n = 5$ WT, 6 KO). **i**–**m** Ex vivo muscle physiology of EDL muscles at 6 months old ($n = 4$ mice/group). WT are 2 Rev-erb^{floxed} mice and 2 MLC-Cre mice. *$p = 0.0458$ by t-test (**j**), 0.0021 (**l**) and 0.0264 (**m**) by 2-way repeated-measure ANOVA. **n**–**s** Treadmill test at 5 months old at the low-speed profile ((**n**–**p**) $n = 15$ WT, 9 KO) or the high-speed profile ((**r**, **s**) $n = 9$ mice/group). WT are Rev-erb^{floxed} mice. *$p = 0.0206$ (p) and 0.0434 (s) by t-test. Data are mean ± SEM unless otherwise specified. ns, not significant.

not found in DEGs involved in glycolysis, ion transport, or adhesion, suggesting that Rev-erb could regulate these genes indirectly through other transcription factors. Consistent with the transcriptome analysis, metabolomics profiling of muscles revealed robust changes in amino acids, glycolytic intermediates, and carnitines between KO and WT muscles, particularly at ZT22 (Fig. 6l). These results demonstrate that muscle Rev-erb regulates time-dependent metabolic and bioenergetics processes.

Muscle Rev-erb regulates muscle fuel metabolism and bioenergetics

The integrated multi-omics analysis suggests increased fatty acid oxidation and BCAA catabolism but reduced glycolysis in KO muscles compared to WT (Fig. 7a). This could contribute to fatigue resistance and low strength in KO muscles since fatty acids are a more efficient fuel for low-intensity exercise, while glucose is preferred for high-intensity exercise. To assess metabolic kinetics, we used primary myocytes as the in vitro model for isotope tracer studies as previously

described[65]. Myocytes from Rev-MKO mice show lower glucose uptake (Fig. 7b) and higher fatty acid oxidation (FAO) (Fig. 7c), supporting the muscle-autonomous fuel preference for lipids over glucose. Using ^{3}H-palmitate as an in vivo tracer during treadmill running as described[65], we found that KO mice display an increased fatty acid oxidation rate during exercise, particularly before sleep (Fig. 7d). Consistent with kinetic analyses, KO mice show reduced muscle triglycerides (TG) content (Fig. 7e), higher muscle and liver glycogen content (Fig. 7f, g), lower blood lactate (Fig. 7h), impaired glucose tolerance (Fig. 7i, j), and increased insulin resistance (IR) as assessed by homeostatic model assessment index for insulin resistance (HOMA-IR) (Fig. 7k) compared to WT mice immediately after treadmill exercise, with all the differences more pronounced at ZT23-1 than at ZT11-13. RER from indirect calorimetry can assess fuel preference during exercise at a higher temporal resolution. KO mice showed a reduced rate of intensity-dependent increase in RER than WT at ZT0 but not at ZT12 (Fig. 7l, m). These results demonstrate that the diurnal variation in exercise-induced fuel preference adaptation is controlled by the
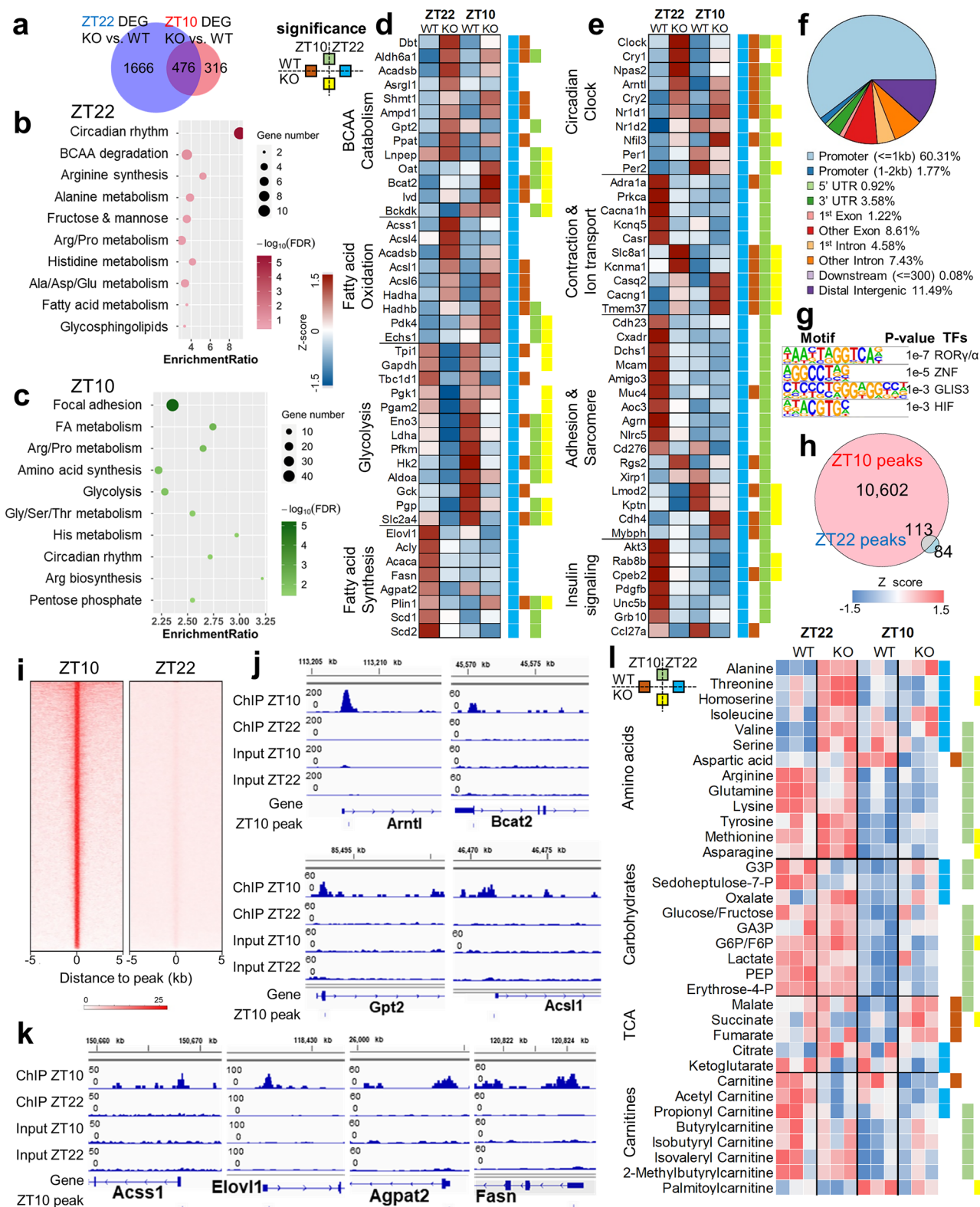
Fig. 6 | Multi-omics characterization of muscle Rev-erb functions. a Venn diagram showing the ZT22 and ZT10 overlap of differentially expressed genes (DEGs) in KO vs. WT as identified by RNA-seq at 6 months of age ($q < 0.05$, fold change > 1.5). WT are Rev-erb[floxed] mice. **b, c** Top enriched KEGG pathways in DEGs at ZT22 and ZT10. **d, e** Heat map of DEGs showing the relative abundance (in Z-score) involved in glycolysis, TCA cycle, fatty acid metabolism, BCAA metabolism, circadian clock, muscle contraction, adhesion, sarcomere, and insulin signaling. **f** Pie chart representing the genomic distribution of Rev-erbα ChIP-seq peaks. **g** Top enriched motif of Rev-erbα peaks at ZT10. **h** Venn diagram showing the overlap of Rev-erbα binding peaks at ZT10 and ZT22. **i** Heat map of Rev-erbα ChIP-seq signals at ZT10 and ZT22. **j, k** Browser tracks of Rev-erbα peaks at genes involved in metabolism. **l** Metabolomics heat map showing the relative abundance (in Z-score) of metabolites at the indicated ZT in quadriceps muscle at 10 months of age ($n = 3$ mice per group). WT are Rev-erb[floxed] mice. Statistical differences were determined using 2-way ANOVA followed by the Tukey test and were indicated on the right side by colors as illustrated in the color key.
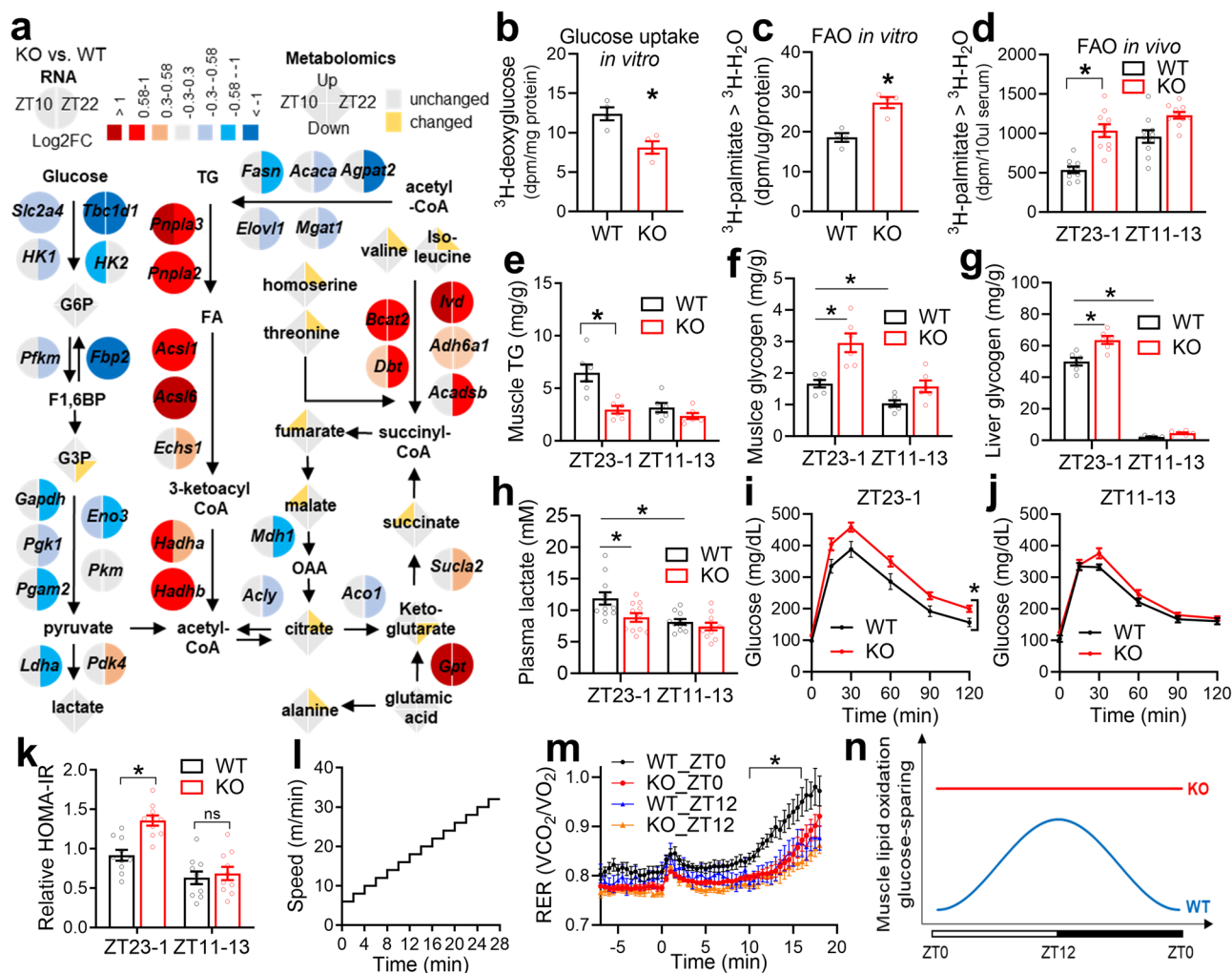
Fig. 7 | Muscle Rev-erb regulates the diurnal rhythm of bioenergetics and time-dependent metabolic adaptations to acute exercise. a Integrated transcriptomics and metabolomics analysis. **b, c** Glucose uptake and fatty acid oxidation (FAO) rates in primary myotubes isolated from mice at 3 months old, followed by electric pulse stimulation (EPS) during isotope tracing with ^{3}H-deoxyglucose (DOG) or ^{3}H-palmitate ($n = 4$ wells of cells from 3 mice/group). WT are Rev-erb^{floxed} mice. *$p = 0.0098$ (**b**) and *$p = 0.0027$ (**c**) with student t-test. **d** FAO rate measured by blood ^{3}H·H$_2$O at 20 min after intraperitoneal injection of ^{3}H-palmitate. Mice at 6 months old were running treadmill at 10 m/min during tracing ($n = 10$ mice/group). WT are 7 Rev-erb^{floxed} and 3 MLC-Cre mice. *$p = 0.0001$ by 2-way ANOVA and Holm-Sidak test. **e–g** Muscle triglycerides (TG), muscle glycogen, and liver glycogen at 5 months old ($n = 6$ mice/group). WT are 3 Rev-erb^{floxed} and 3 MLC-Cre mice. *$p = 0.0002$ (**e**), 0.0002 (WT vs. KO at ZT23-1) and 0.0276 (ZT23-1 vs. ZT11-13 for

WT) for (**f**), and 0.0001 (**g**) by 2-way ANOVA and Holm-Sidak test. **h** Blood lactate after a bout of treadmill exercise at 4 months old ($n = 11$ mice/group). WT are 9 Rev-erb^{floxed} and 2 MLC-Cre mice. *$p = 0.0081$ (WT vs. KO at ZT23-1) and 0.0027 (ZT23-1 vs. ZT11-13 for WT) by 2-way repeated-measure ANOVA and Holm-Sidak test. **i, j** GTT at 10 months old after running at 12 m/min speed for 25 min ($n = 10$ WT, 11 KO). *$p = 0.0101$ for genotype effects with 2-way repeated-measure ANOVA. WT are 8 Rev-erb^{floxed} and 2 MLC-Cre mice. **k** HOMA-IR at 10 months old ($n = 10$). WT are 8 Rev-erb^{floxed} and 2 MLC-Cre mice. *$p = 0.0004$ by 2-way ANOVA and Holm-Sidak test. **l, m** Speed profile and RER during a bout of treadmill exercise at 9 months old ($n = 8$ mice/group). WT are 6 Rev-erb^{floxed} and 2 MLC-Cre mice. *$p = 0.0013$ (WT_ZT0 vs. KO_ZT0) for genotype effects by 2-way repeated-measure ANOVA. **n** A working model of muscle fuel metabolic rhythmicity. Data are mean ± SEM. ns, not significant.

muscular clock rather than passive responses to food. Thus, the drop of Rev-erb before sleep anticipates the metabolic needs of sleep by promoting muscular fatty acid oxidation while sparing glucose, which contributes to the enhanced fatigue resistance upon waking (Fig. 7n). Conversely, the low fatigue resistance before sleep could lead to more profound hormetic compensatory adaptations to exercise[66,67], contributing to better muscle functions in chronic exercise training before sleep than upon waking. Thus, Rev-erb-dependent metabolic remodeling underlies both the baseline diurnal variations and time-dependent effects of chronic training in muscle contractile functions.

Discussion

What is the best time of the day for exercise? Since evening (PM) is the end of the sleep phase for mice, while morning (AM) is the beginning of the sleep phase, our mouse studies suggest that engaging in low-

intensity exercise before sleep yields greater efficacy than exercising after waking in reducing body weight, enhancing muscle strength and endurance, and improving glucose tolerance. These results are consistent with recent studies suggesting that exercise training during the early sleep or late wake phases superior endurance adaptations or weight loss compared to training during the late sleep or early wake phases in mice[68,69].

What molecular mechanisms drive the timing effects of exercise training? Weight loss results from an imbalance between energy intake and expenditure. We found no differences in total food intake between exercise before and after sleep. Instead, we found that exercising after waking reduced spontaneous locomotor activity and energy expenditure during the subsequent wake cycle compared to exercising before sleep. At first glance, it seemed these effects depended solely on sleep timing. For exercise before sleep, since the post-training rest

temporarily aligns with the normal sleep cycle, it would not alter the spontaneous locomotor activity the next day. Conversely, for exercise training after waking, its post-training rest interferes with the otherwise active locomotor activity, partially offsetting the exercise effects on total energy expenditure. However, this interpretation is refuted by the fact that Rev-MKO mice, despite normal sleep/wake cycles and rhythmic energy expenditure at the baseline, did not show timing-dependent effects of exercise on suppressing spontaneous locomotor activities or energy expenditure. What muscle-intrinsic factor downstream of Rev-erb accounts for training time-dependent activity-suppressive effects? Muscle fatigue resistance appears to be the answer because baseline muscle exercise capacity before sleep is lower than after waking, a pattern abolished in the absence of muscular Rev-erb.

How does Rev-erb regulate endurance or fatigue resistance? Aside from weight loss, what causes timing-specific effects of training on muscle strength and systemic glucose tolerance? Unbiased multiomics analyses suggest that the muscular bioenergetics process likely plays a significant role. Muscles burn more glucose while awake and more lipids during sleep. Such diurnal flexibility is locked by Rev-erb deletion into a state that constantly favors lipids over glucose. Since Rev-erb levels rise in the late sleep phase, anticipating the upcoming wake phase, Rev-erb depletion produces the maximum effects of promoting lipid oxidation and sparing glucose before sleep. The heightened preference and efficiency for lipid oxidation in Rev-MKO mice are supported by metabolic tracing analyses and could explain the enhanced exercise endurance, as lipids constitute a larger energy reservoir than carbohydrates and are preferred for low-intensity exercise. The impaired glucose uptake in the absence of Rev-erb, validated by tracing analyses and metabolic measurements, likely contributes to the reduced muscle strength and impaired glucose tolerance in Rev-MKO mice compared to WT mice. Importantly, muscle-specific disruption of Rev-erb blunts baseline diurnal variations in muscle strength, endurance capacity, and systemic glucose tolerance, which is associated with enhanced endurance but impaired glucose tolerance at the late wake phase. Thus, the time-dependent regulation of fuel metabolism by muscle Rev-erb plays a crucial role in both the baseline metabolic rhythm and diurnal variations of adaptations to exercise training.

Why do some phenotypes in KO mice match the WT_AM while others match WT_PM? Since Rev-erb suppresses FAO and promotes carbohydrate utilization. The rise of Rev-erb in the late sleep phase likely anticipates and facilitates the transition from sleep to wakefulness, favoring carbohydrate use. In the KO mice, the loss of Rev-erb locks the muscle into a "sleep-like PM state" that prioritizes fatty acid oxidation over carbohydrate metabolism. Since FAO-powered contraction is more fatigue-resistant while glycolysis supports peak contractile force, this metabolic shift could explain why KO mice resemble WT_PM (ZT11-13) rather than WT_AM (ZT23-1) in grip strength, wire hang, torque, fatigue, muscle triglycerides, plasma lactate, post-exercise glucose tolerance, and baseline exercise-induced RER. Similarly, after chronic training, KO mice remain more similar to WT_EX_PM than WT_EX_AM in grip strength, wire hang, glucose tolerance, torque, and fatigue. The preference of KO muscle for fatty acids likely suppresses training-induced upregulation of carbohydrate metabolism and the subsequent anabolic remodeling of muscle contractile machinery. This may explain why KO and WT_EX_PM, compared to WT_EX_AM, show greater resistance to training-induced improvements in muscle contractile performance and glucose tolerance. Intriguingly, KO mice align more closely with WT_EX_AM than WT_EX_PM in body weight. The higher baseline fatigue resistance in KO mice might mitigate the PM training-induced suppression of spontaneous locomotor activity during wakefulness. Unlike PM training, AM training is followed by sleep and does not reduce total spontaneous activity and energy expenditure in either genotype. As a result, KO mice resemble WT_EX_AM in maintaining higher total energy

expenditure during chronic training, potentially accounting for their lower body weight. KO mice also align more closely with WT_EX_AM than WT_EX_PM in the graded treadmill exercise test. Multiple factors could contribute to this outcome, including the lower body weight of KO mice and differences in treadmill speed influencing the KO vs. WT comparisons. Beyond fuel metabolism and bioenergetics, other biological processes, such as amino acid metabolism, ion channel function, extracellular matrix composition, and sarcomere dynamics, may play a role. Finally, chronic training at a fixed time of day could alter the oscillatory pattern of muscle clock gene expression, another layer of complexity that warrants future investigation.

One surprising finding from our study is regarding the role of feeding in muscle metabolic adaptations to exercise training. Feeding is known to promote lipid synthesis, enhance carbohydrate utilization, and suppress systemic fatty acid oxidation, characterized by a higher respiratory ratio in feeding than in fasting in normal physiology[70]. Since food intake is well known to have a diurnal rhythm, a diurnal variation in exercise-induced substrate utilization or fuel preference is widely believed to be driven by feeding conditions. Our results challenge this prevailing view because the timing effects of chronic exercise in body weight, muscle contractile performance, and glucose tolerance are all abolished in Rev-MKO mice undergoing the same exercise training regimen even though they have normal feeding patterns. Therefore, the Rev-erb-mediated muscle-specific anticipatory mechanism, but not the diet-induced responsive mechanism, is essential for diurnal variations of systemic metabolic adaptations to exercise.

The metabolic profile observed in Rev-MKO mice aligns with findings from several other genetic mouse models of the circadian clock. Rev-MKO mice show some similarities to mice with skeletal muscle-specific knockout of Bmal1 (Bmal1-MKO)[61,71]. (1) Both mouse lines show the normal daily distribution of feeding time and total food intake, suggesting the muscle clock does not affect feeding rhythm. (2) Both mouse lines increased fatty acid oxidation. Bmal1-MKO mice show upregulated genes in oxidative metabolism[71,72], increased oxidative capacity, and improved endurance[73]. (3) Both mouse lines show reduced glucose uptake and downregulated glycolysis gene expression[61,74]. In vitro studies with Bmal1 null myotubes also demonstrated impaired glycolysis[34]. (4) Both mouse lines show reduced muscle TG, elevated muscle BCAA content, and reduced muscle force compared to their WT control. There are also differences: (1) Bmal1-MKO mice display no difference in endurance compared to WT controls, while Rev-MKO mice exhibit enhanced endurance under low-speed exercise conditions. (2) Bmal1-MKO mice exhibit increased energy expenditure compared to WT, while Rev-MKO mice show no significant changes in energy homeostasis at the baseline. (3) Bmal1-MKO mice show normal glucose tolerance, while Rev-MKO mice experience impaired glucose tolerance after treadmill exercise. (4) Bmal1-MKO mice have a higher percentage of lean mass and lower fat mass, while body composition in Rev-MKO mice remained unchanged at the baseline. Therefore, Bmal1 and Rev-erb are both essential for muscles to anticipate the energy supply and demand oscillations but may regulate partially different metabolic pathways.

Rev-erb recruits nuclear receptor co-repressor (NCOR) and histone deacetylase 3 (HDAC3) for transcription repression[75]. The Rev-MKO phenotype is also in keeping with the boosted oxidative metabolism and enhanced exercise endurance in the NCOR1 muscle-specific knockout mouse model[76], as well as the shift from glucose utilization to lipid oxidation observed in the HDAC3 muscle-specific knockout mouse model, as we previously reported[54]. Depletion of muscle HDAC3 or abolishing its enzyme activity compromised muscle strength but enhanced fatigue resistance[54,65]. Given that Bmal1 regulates the transcription of other core clock genes besides Rev-erb, and NCOR/HDAC3 modulate numerous nuclear receptors beyond Rev-erb,

manipulating Bmal1 or NCOR/HDAC3 may have broader implications than Rev-erb depletion alone and does not predict the role of muscular Rev-erb. The current study fills this knowledge gap. The consistent effects between muscle-specific knockout of Rev-erb and those of Bmal1 and NCOR/HDAC3 suggest that Rev-erb plays a significant role in mediating the metabolic functions of Bmal1 and NCOR/HDAC3 in skeletal muscles.

Prior studies[19,77] with global knockout of Per1/2 or Bmal1 demonstrated baseline diurnal variation in exercise capacity, defined by the rate of blood glucose decline or liver glycogen depletion during an acute treadmill exercise bolus. However, it remains unknown whether chronic exercise training at different times of the day has distinct effects on muscle contractile performance or glucose tolerance. Since the circadian clock operates in nearly all tissues, global knockout models do not identify which tissues are responsible for the baseline diurnal variation or the timing-dependent effects of chronic exercise training. Specifically, as the global knockout of Per1/2 or Bmal1 abolishes the feeding diurnal rhythm, whether feeding rhythms drive the baseline rhythmic response to a bolus exercise is unclear. Our current study addressed these questions and demonstrated that the muscle clock, rather than the central clock or the feeding rhythm, governs the variation in baseline responses to acute exercise and adaptations to chronic exercise training.

The Rev-MKO mice exhibit normal muscle mitochondrial content, locomotor activity, and food intake, which contrasts with whole-body Rev-erbα or Rev-erbβ null mice displaying reduced muscle mitochondrial content or locomotor activity[38], or altered food intake[40]. This disparity may stem from non-muscular systemic effects in global null mice, potentially contributing to mitochondrial content abnormalities and muscle atrophy[38,39]. For instance, over 85% reduction in spontaneous activity in Rev-erbα null mice could independently induce muscle atrophy[38,39]. Similarly, increased food consumption during the light cycle in Rev-erbβ null mice might indirectly influence muscle glucose metabolism[40]. Another explanation could be that the truncated Rev-erbα protein retains some functionality. However, knockdown of Rev-erbβ in cultured myotubes has been shown to increase the expression of fatty acid oxidation genes[40], consistent with our findings. Intriguingly, loss-of-function of muscle-specific Rev-erb increases endurance during low-intensity exercise and enhances fatty acid oxidation without altering mitochondrial content, while Rev-erb gain-of-function with agonists also boosts muscle mitochondrial oxidative capacity and enhances exercise performance[39,44,45]. Contrary to the assumption that loss and gain of function have opposite effects, Rev-erb gain-of-function and loss-of-function do not necessarily exhibit opposing effects in cultured myotubes[40,78]. Moreover, it is plausible that systemic factors, rather than solely muscle-autonomous effects, contribute to the beneficial effects of Rev-erb-targeting small molecules. Nonetheless, the characterization of Rev-MKO mice suggests that muscle Rev-erb can modulate contractile functions and bioenergetics without affecting muscle mitochondrial content.

While the current study focuses on metabolism and bioenergetics, non-metabolic processes can also contribute to the timing effects of chronic exercise training[79]. Genes associated with contraction, ion transport, adhesion, sarcomere organization, and insulin signaling are also significantly regulated by muscle Rev-erb and display a robust diurnal rhythm in muscles under normal conditions. Identifying the muscle clock gene Rev-erb as essential for controlling these timing effects opens avenues for further dissecting the underlying mechanisms, which will shed light on the optimal exercise training regimen.

The current study has several limitations. (1) Our study found that long-term treadmill exercise before sleep improved muscle contractile functions and systemic glucose metabolism more effectively than exercise immediately after awakening. However, since we focused on prolonged, low-intensity running, these results may not apply to those performing high-intensity workouts for weight loss or to elite athletes whose training differs in intensity and goals. Further research is needed to determine if the time-of-day impact observed here extends to higher-intensity or performance-focused exercise routines. (2) Since circadian clock genes are intricately interlocked in negative feedback loops, the depletion or overexpression of one clock gene inevitably affects the expression of others. As a result, current technology does not allow us to distinguish between direct and indirect effects clearly. Therefore, we interpret the results at face value − if knocking out Rev-erb induces changes, we attribute those changes to Rev-erb without claiming they are direct effects. (3) Since clock genes could have clock-independent functions, it is unknown whether the observed function of muscular Rev-erb is dependent on the clock function. However, the following evidence supports a clock-dependent role of Rev-erb for outcomes observed in our study. (a) Rev-MKO mice show no developmental defect, with normal body weight, body size, muscle fiber number, fiber diameter, fiber composition, and mitochondrial content with both mitochondrial DNA copy number and OXPHOS protein levels. (b) The baseline phenotypic differences between Rev-MKO and WT mice, including exercise endurance and strength, are dependent on the measurement time (morning vs. evening). (c) The post-exercise differences between Rev-MKO and WT mice, including muscle glycogen, fatty acid oxidation, muscle TG, blood lactate, and glucose tolerance, are also dependent on the measurement time concordant with the time point with a maximum transcriptomic difference. These data suggest that the observed phenotypic changes between KO and WT are likely due to the clock-related function of Rev-erb. Future studies with phase-specific re-expression rescue experiments are needed to clarify this point.

Methods
Animals
The animal care and use procedures followed the Institutional Animal Care and Use Committee guidelines at Baylor College of Medicine. The experiments conducted in the present study were reviewed and approved by the Institutional Animal Care and Use Committee (IACUC) of Baylor College of Medicine. Animals were monitored daily for signs of distress, including weight loss, lethargy, abnormal posture, or reduced mobility. Humane endpoints were predefined, and animals exhibiting severe or unrelieved distress were euthanized using CO_2 inhalation followed by cervical dislocation following the American Veterinary Medical Association (AVMA) guidelines to ensure a humane death. The muscle-specific Rev-erb knockout mice (Rev-MKO) were generated by crossbreeding mice bearing Rev-erbα[loxP] (Nr1d1[tm1.2Rev], MGI ID 5426700) and Rev-erbβ[loxP] (Nr1d2[tm1.1Rev], MGI ID 5426699) alleles[55,80] with the MLC-Cre line (MGI ID 1931135)[56]. The resultant Rev-MKO mouse line has been backcrossed to the C57BL/6 J background for over five generations. Littermate mice bearing Rev-erbα[loxP]/Rev-erbβ[loxP] alleles (referred to as Rev-erb[floxed]) without Cre or the Cre allele without Rev-erbα/β[loxP] (referred to as MLC-Cre) were used as the wild-type (WT) control and indicated in the figure legends. Male mice at the age of 2 months to 10 months were used. The ages of each experiment were indicated in figure legends. All animals were housed under a 12-h day/night cycle at $22 \pm 2\,°C$, with humidity of $60\% \pm 5\%$. Zeitgeber time 0 (ZT0) indicates light-on (7:00 AM), and ZT12 indicates light-off (7:00 PM) under the normal light-dark (LD) cycle. We abide by the ARRIVE guidelines for reporting of animal experiments.

Grip strength and wire hang tests
A Bioseb meter was used to measure forelimb grip strength as described previously[53,81]. Briefly, mice were pulled by the base of the tail parallel to the bar. After holding the bar, they were pulled backward horizontally and gently at a constant speed until the grip was released.

Five trials were taken continuously for a session, and at least five sessions were performed with at least a 5 min rest interval between each session. The top three highest readings from any of these trials were averaged for the mouse. For the baseline study, the tests were conducted at ZT23-1 and ZT11-13, respectively. For the timing effects of chronic exercise, we conducted experiments at least 12 h after a routine training session to avoid the impact of acute exercise on muscular fatigue. For the wire hang test, mice were horizontally suspended and upside down on a metal wire mesh (2 mm in diameter and 1 m in length) 50 cm above a landing surface filled with soft bedding[53]. The time when the animal fell was recorded, and the results were represented as body weight as hanging time (s) × body weight (g). Three trials were conducted per animal on average, with a 5 min rest period between each trial. For the baseline study, the tests were conducted at ZT23-1 and ZT11-13, respectively. For the timing effects of chronic exercise, we conducted experiments at least 12 h after a routine training session to avoid the impact of acute exercise on muscular fatigue.

Treadmill exercise test and training

Graded exercise test was performed using an Exer 3/6 Treadmill with an electrical stimulus system and the automatic stimulus detection unit (Columbus Instruments) as previously described with some modifications[54]. Mice were motivated to run by electric shocks at 1 Hz with a stimulation intensity of 3, without inclination. The shocks at such intensity and frequency were well-tolerated by mice. No mice showed injury after testing or training. Two different speed profiles were used for endurance tests. For the low-speed profile, after mice were placed on the stationary treadmill for 5 min, the treadmill started at 6 m/min, the speed was increased by 2 m/min every 10 min, then 30 min for 18 m/min, 15 min for 20, 22, 24, with no further increase in speed beyond 26 m/min. The high-intensity profile required mice to run on the treadmill at 10 cm/s for 4 min followed by an incrementing speed of 2 cm/s every 2 min. Exhaustion was defined as the time when the mouse reached 50 cumulative shocks for the entire test. Each mouse was allowed a maximum of 50 shocks. Once the cumulative shocks for a specific lane reached 50, the shocking unit for that lane automatically turned off. At this point, the mouse in that lane could rest on the shocking grid while the treadmill continued running. Mice were then removed from the treadmill after all lanes had finished. For long-term exercise training, mice were subjected to treadmill running for 1 h at 10 m/min, without inclination, every other day, either in the morning at ZT23-1 (EX_AM) or in the evening at ZT11-13 (EX_PM). The sedentary control group was placed on a stationary treadmill for the same duration at any time.

In vivo muscle physiology

Muscle physiological analysis was performed on the dorsi flexor tibialis anterior (TA) muscles using an Aurora Mouse 1300 A 3-in-1 Whole Animal System equipped with Dynamic Muscle Control v.5.501 software as previously described[57–59]. Briefly, the hind limb hair was shaved and cleaned, and the anesthetized mouse was positioned in a supine position with the head secured on a heated platform with an oxygen flow rate of 1 L/min supplemented with 2.5% isoflurane. The electrode was placed subcutaneously 2–4 mm beneath the skin directly over the TA muscle and recorded the lowest current at which the highest twitch torque was achieved. This determined the optimal current to be used for the torque-frequency experiment. Maximal isometric twitch and tetanic contractions were obtained using a stimulation frequency of 100 Hz for 500 msec. Five minutes were allowed between two tetanic contractions to ensure muscle recovery. For induction of fatigue, muscles were stimulated every five seconds for 90 contractions using 40 Hz pulses lasting 300 ms. The tetanic strength and fatigue resistance are expressed as torque mN•m (millinewton meters).

Ex vivo muscle physiology

Ex vivo assessment was performed by the Muscle Physiology Assessment Core of the University of Pennsylvania, as we previously described[54,65]. Muscle physiological analysis was performed on isolated EDL muscles using an Aurora Mouse 1200 A System equipped with Dynamic Muscle Control v.5.415 software. EDL muscles were maintained in continuously oxygenated Ringer's solution (100 mM NaCl, 4.7 mM KCl, 3.4 mM CaCl2, 1.2 mM KH2PO4, 1.2 mM MgSO4, 25 mM HEPES and 5.5 mM d-glucose) at 24 °C. The twitch stimulation protocol applied was a single stimulus with a duration of 0.2 ms. For measuring tetanic maximal force generation, the stimulus was repeated at a frequency of 120 Hz for 500 ms. Five min were allowed between two tetanic contractions to ensure muscle recovery. For induction of fatigue, 5 min after the last maximal tetanic contraction, muscles were stimulated every second for 8 min using 40 Hz pulses lasting 330 ms. The fatigue index was expressed as the percentage difference in force between the first contraction and every subsequent contraction for EDL or as the percentage of force left after the preceding contraction. Following the fatigue protocol, a burst of 50 maximal tetanic contractions (120 Hz for 500 ms) was applied to ensure complete fatigue across all samples. The recovery protocol started 1 s after the last burst contraction. A maximal tetanic stimulation (120 Hz for 500 ms) was given every 5 min for 30 min, and the force recovery was expressed as a percentage of the maximal isometric tetanic force.

Indirect calorimetry

Indirect calorimetry was performed using the most recent Comprehensive Lab Animal Monitoring System (Oxymax/CLAMS-HC, Columbia instruments). Briefly, the individual animal was acclimated to a metabolic chamber equipped with a running wheel on the system for at least 1.5 days prior to analysis. During the monitoring period, O_2 and CO_2 levels were collected every 20 min over several days. For the timing effects of chronic exercise, mice were taken out twice for treadmill training according to their established exercise schedule during over 5 days of monitoring, and the missing data due to the brief disruption was not included in the final statistics. Data on locomotor activity and food intake were measured in real time. Data was not normalized to body weights unless otherwise stated.

Immunofluorescence and Western blot

Fresh tibialis anterior (TA) muscles were isolated, embedded in OCT compound, and frozen in the dry ice-chilled isopentane. Cross-sections at 10 μm thickness were obtained using a Leica CM1850 cryostat. Tissue sections were incubated with mixed primary antibodies: laminin (Sigma), MHC-IIa (2F7; Developmental Studies Hybridoma Bank), and MHC-IIb (BF-F3; Deutsche Sammlung von Mikroorganismen und Zellkulturen) in blocking buffer, followed by incubation with secondary antibodies: Alexa-647-goat anti-rabbit, Alexa-594-goat anti-mouse IgG, and Alexa-488-goat anti-mouse IgM (A32733, A21121, A21426; Invitrogen, dilution: 1:1000 in PBS). Unstained fibers were counted as MHC-IIX, based on the fact that mouse TA muscles contain few type I fibers[82]. Fluorescent images were captured with a Zeiss Axiophot epifluorescence microscope and Axiovision software. For western blot, tissues were lysed in RIPA buffer, which contained PMSF and proteinase inhibitor. The concentration of total protein was quantified using Bradford protein assay. Lysates were resolved on SDS-PAGE gel electrophoresis and then transferred to PVDF membranes. The membranes were further treated with skimmed milk and blotted with antibodies of Hsp90 (CST 4874) and OXPHOS proteins (MitoSciences MS604).

Glucose tolerance and metabolite measurement

Glucose tolerance tests (GTT) were performed at ZT23-1 and ZT11-13 after fasting for 8 h. D-(+)-glucose was intraperitoneally injected at 1.5 g/kg or 2 g/kg. Blood samples were obtained from the tail vein and

measured repeatedly by glucometer (OneTouch) at 0, 15, 30, 60, 90, and 120 min after glucose injection. For measuring hepatic and muscle glycogen, frozen mouse liver (~50 mg) and quadriceps muscle (~500 mg) samples were digested in 30% KOH at 60 °C for 20 min. Ethanol and 6% Na$_2$SO4 were then added to samples to precipitate glycogen overnight at −20 °C, followed by centrifugation at 3000 rpm for 10 min at 4 °C. Glycogen was resuspended in 150 μL of acetate buffer (0.2 M pH 4.8). Glycogen was precipitated by ethanol and digested with 0.25 mg/ml amyloglycosidase (Sigma-Aldrich), followed by glucose assay using HK kit (Sigma-Aldrich). All samples were measured in triplicates along with glucose standards. For measuring blood lactate, plasma samples were collected from the tail at ZT0 and ZT12 after subjecting mice to an acute single bout of treadmill running at 18 m/min for 20 min. L-lactate levels were measured calorimetrically using a colorimetric kit (Sigma Scientific, St. Louis, Missouri). For measuring muscle triglycerides, mice were sacrificed by cervical dislocation either after a 10 h fasting period or after refeeding (6 h fasting, 4 h refeeding). Quadriceps were homogenized in the tissue lysis buffer (140 mM NaCl, 50 mM Tris, and 0.1% Triton-X). Muscular triglyceride levels were measured using the Stanbio LiquiColor® Triglycerides kit (*Stanbio*, Boerne, Texas). All assays were performed in triplicate with external standards included in each run.

qPCR and RNA-Seq

For mitochondrial DNA copy number, total genomic DNA extracted from the muscles were analyzed by qPCR with primers specific to a mitochondrial gene (mtND1) and normalized to LPL (a gene coded on nuclear genome). For RT-qPCR or RNA-seq, total RNA was extracted using TRIzol (Invitrogen) and a High Pure RNA tissue kit (Roche). RT-qPCR was performed with High Capacity RT kit, SYBR Green PCR Master Mix, and the Quant Studio 6 instrument (Life Science) using an absolute quantification method with standard curves. 18S RNA was used as the housekeeping control. For the sequence primers, see Supplementary Information. RNA-seq was performed using total RNA extracted from Tibialis anterior in mice at 6 months of age ($n = 3$ at each condition, total of 12 samples). RNA-seq analysis was performed as described previously[83] RNA was isolated using Trizol reagent (Sigma) followed by RNeasy Mini Kit (Qiagen). The KO vs. WT samples were sequenced on the BGI MGISEQ-2000 platform with PE100 and 6 Gb total clean reads per sample. Raw reads were subjected to SOAPnuke (v1.5.2) processing to remove sequencing adapters and low-quality reads. The clean reads were mapped to the mouse genome (GRCm38.p6) via HISTA2 (V2.0.4). The gene expression level was calculated using Bowtie2 (V2.2.5) and RSEM (V1.2.12). Differential expression analyses were conducted via DESeq2 package (V1.4.5). The KEGG and GO enrichment analysis was performed by *clusterProfiler*.

Metabolomics

Quadriceps were harvested from male mice at 10 months of age ($n = 3$ at each condition) and snap-frozen in liquid nitrogen. Metabolites were extracted as previously described methods[83]. Data were acquired in multiple reaction monitoring (MRM) using Agilent QQQ LC-MS systems. Separation of TCA and glycolysis metabolites were performed using 5 mM ammonium acetate in water as buffer pH 9.9 (A), and 100% acetonitrile as buffer (B) using Luna 3 μM NH2 column (Phenomenex, Torrance, CA) and measured 6495 Triple Quadrupole mass spectrometer via ESI negative mode (Agilent Technologies, Santa Clara, CA). The Gradient used is as follows: 0–20 min-80% B (Flow rate 0.2 ml/min); 20-20.10 min- 80% to 2% B; 20.10-25 min-2% B (Flow rate 0.3 ml/min); 25–30 min 80% B (Flow rate 0.35 ml/min); 30–35 min-80%B (Flow rate 0.4 ml/min); 35-37.80 min 80% B (Flow rate 0.4 ml/min); followed by re-equilibration at the end of the gradient to the initial starting condition 80% B at Flow rate of 0.2 ml/min. Separation and measurement of amino acids and carnitines were performed using Zorbax Eclipse XDB C18, 1.8 micron, 4.6×100 mm column on 6495 triple

quadrupole mass spectrometer via ESI Positive mode (Agilent Technologies, Santa Clara, CA). Mobile phases A and B were 0.1% formic acid in water and acetonitrile, respectively. The gradient used is as follows: 0–6 min−2% of B, 6–6.50 min-30 % B, 6.50–7 min−90% of B, 7–12 min 95% of B,13 min 30% of B followed by re-equilibration at the end of the gradient 20 min to the initial starting condition 2% of B. Flow rate: 0.2 ml/min. The data were analyzed using MetaboAnalyst 6.0, first normalized by internal standards, log transformation, and auto-scaling methods. Statistical differences were determined using 2-way ANOVA followed by Tukey test for multiple comparison corrections. Differential metabolites were identified by *p*-value < 0.05.

ChIP-Seq

Mouse skeletal muscles were harvested at ZT10 and ZT22 (3 male WT mice at 6 months old at each time point). Briefly, tissues were ground in liquid N2 and cross-linked in 1% formaldehyde for 20 min. Whole-cell extracts were sonicated and immunoprecipitated with antibodies to Rev-erbα (Cell signaling, cat # 13418). The precipitated DNA was then pooled and amplified according to the guideline of Illumina, followed by sequencing on illumina nextseq 500 (need to confirm). Sequenced reads were aligned to the mm10 genome using Bowtie 2 (version 2.3.4.2). Non-redundant and uniquely mapped reads were used for downstream analysis. Read coverage for every 50 bp bins was calculated using the bamCoverage function of deepTools (version 3.5.4) function, avoiding blacklist regions of the mouse genome (ENCODE project). Genome browser tracks were visualized in Integrative Genome Browser (IGV version 2.16.1). Peak calling was performed on unique reads with MACS2 using input as control (with parameters −q 0.05 -nomodel --shift -100 --extsize 200). ChIP heatmap plots were generated using computeMatrix (with reference-point mode) and plotHeatmap functions with default settings (deepTools, version 3.5.4). Motif mining was performed using Homer in 200 bp regions surrounding peak centers.

Primary myoblasts and isotope tracing in vitro

Isolation and culturing of primary myoblasts were adapted from the previous report[65]. Briefly, primary myoblasts were extracted from skeletal muscles by mincing and digesting them in a mixture of type I collagenase and Dispase B (Roche Applied Science). Cells were filtered from debris, centrifuged, and cultured in a growth medium (F-10 Ham's medium supplemented with 20% FBS, 5 ng/ml basic fibroblast growth factor, and 1% penicillin-streptomycin) on collagen-coated cell culture plates at 37 °C, 5%CO$_2$. Multiple pre-plating was used to remove fibroblasts. For differentiation into myotubes, when primary myoblasts were around 95% confluency, differentiation media (DMEM supplemented with 2% fetal horse serum and 1% penicillin-streptomycin) was treated for 5 days. Differentiated myotubes and myogenic cells were harvested for further investigations in 7 days, and fresh differentiation medium was added every 2 days. In order to detect the fatty acids oxidation, differentiated myotubes were incubated in PBS and supplemented with [9,10^{3}H(N)]-palmitate, conjugated on BSA and carnitine for 120 min at 37° in the incubator. EPS using the IonOptix C-pace system with 15 volts at 1 Hz was applied 30 min before adding the [9,10-^{3}H(N)]-palmitate. The resultant ^{3}H-H2O in the incubation solution was separated from precursors using ion-exchange columns (DOWEX 1×4–400) as described previously[54]. For cellular glucose uptake, 2-[^{3}H(N)]deoxy-d-glucose was supplemented to cells for 10 min before 6 h serum starvation. Subsequently, the cells were washed three times with cold PBS and lysed in RIPA buffer containing 1% SDS. Radioactivity was measured using a scintillation counter and normalized with the protein concentration of cell lysates.

Statistics

GraphPad Prism 10 software and R software environment were used for statistical analysis. RNA-seq, ChIP-seq, Metabolomics, body

composition, fiber quantification, indirect calorimetry, glucose tolerance test, muscle strength, and muscle fatigue were performed by investigators who were blinded to the mouse genotype. The sample size for each group was indicated in the figures, figure legends, or the methods section above. No statistical methods were used to predetermine sample sizes. Instead, sample sizes were determined based on previous publications. Data were analyzed using ANOVA or unpaired Student's t-test as specified in details in the figure legends. All statistical analyses and SEM calculations were based on individual mice unless otherwise indicated in the figure legends. All attempts at replication were successful. Normality was tested by the Shapiro-Wilk test. All tests were two-sided.

Reporting summary

Further information on research design is available in the Nature Portfolio Reporting Summary linked to this article.

Data availability

RNA-sequencing data (GSE249730) and chromatin immunoprecipitation sequencing data (GSE263635) are available in Gene Expression Omnibus (GEO). Metabolomics data are available on the National Metabolomics Data Repository (NMDR) website, Study ID: ST003258, Project https://doi.org/10.21228/M87V6Z. Source data are provided as a Source Data file. All data generated for this study will be made available from the corresponding author upon request for reproducibility purposes. Source data are provided with this paper.

References

1. Cartee, G. D., Hepple, R. T., Bamman, M. M. & Zierath, J. R. Exercise promotes healthy aging of skeletal muscle. *Cell Metab.* **23**, 1034–1047 (2016).
2. Distefano, G. & Goodpaster, B. H. Effects of exercise and aging on skeletal muscle. *Cold Spring Harb. Perspect. Med.* **8**, a029785 (2018).
3. Steele, J. et al. Slow and steady, or hard and fast? A systematic review and meta-analysis of studies comparing body composition changes between interval training and moderate intensity continuous training. *Sports Basel Switz.* **9**, 155 (2021).
4. van der Velde, J. H. P. M. et al. Timing of physical activity in relation to liver fat content and insulin resistance. *Diabetologia* **66**, 461–471 (2023).
5. Qian, J. et al. Association of timing of moderate-to-vigorous physical activity with changes in glycemic control over 4 years in adults with type 2 diabetes from the look ahead trial. *Diabetes Care* **46**, 1417–1424 (2023).
6. Sabag, A. et al. Timing of moderate to vigorous physical activity, mortality, cardiovascular disease, and microvascular disease in adults with obesity. *Diabetes Care* **47**, 890–897 (2024).
7. Feng, H. et al. Associations of timing of physical activity with all-cause and cause-specific mortality in a prospective cohort study. *Nat. Commun.* **14**, 930 (2023).
8. Blankenship, J. M. et al. Examining the role of exercise timing in weight management: a review. *Int. J. Sports Med.* **42**, 967–978 (2021).
9. Brito, L. C. et al. Chronobiology of exercise: evaluating the best time to exercise for greater cardiovascular and metabolic benefits. *Compr. Physiol.* **12**, 3621–3639 (2022).
10. Bruggisser, F. et al. Best time of day for strength and endurance training to improve health and performance? A systematic review with meta-analysis. *Sports Med. Open* **9**, 34 (2023).
11. Galan-Lopez, P. & Casuso, R. A. Metabolic adaptations to morning versus afternoon training: a systematic review and meta-analysis. *Sports Med. Auckl. NZ* **53**, 1951–1961 (2023).
12. Mancilla, R. et al. Exercise training elicits superior metabolic effects when performed in the afternoon compared to morning in metabolically compromised humans. *Physiol. Rep.* **8**, e14669 (2021).
13. Arciero, P. J. et al. Morning exercise reduces abdominal fat and blood pressure in women; evening exercise increases muscular performance in women and lowers blood pressure in men. *Front. Physiol.* **13**, 893783 (2022).
14. Chiang, S.-L. et al. Effects of a 12-week moderate-intensity exercise training on blood glucose response in patients with type 2 diabetes: A prospective longitudinal study. *Med. (Baltim.)* **98**, e16860 (2019).
15. Souissi, N., Gauthier, A., Sesboüé, B., Larue, J. & Davenne, D. Effects of regular training at the same time of day on diurnal fluctuations in muscular performance. *J. Sports Sci.* **20**, 929–937 (2002).
16. Chtourou, H. et al. The effect of training at the same time of day and tapering period on the diurnal variation of short exercise performances. *J. Strength Cond. Res.* **26**, 697–708 (2012).
17. Teo, S. Y. M., Kanaley, J. A., Guelfi, K. J., Marston, K. J. & Fairchild, T. J. The effect of exercise timing on glycemic control: a randomized clinical trial. *Med. Sci. Sports Exerc.* **52**, 323–334 (2020).
18. Sato, S. et al. Time of exercise specifies the impact on muscle metabolic pathways and systemic energy homeostasis. *Cell Metab.* **30**, 92–110.e4 (2019).
19. Ezagouri, S. et al. Physiological and molecular dissection of daily variance in exercise capacity. *Cell Metab.* **30**, 78–91.e4 (2019).
20. Pendergrast, L. A. et al. Metabolic plasticity and obesity-associated changes in diurnal postexercise metabolism in mice. *Metabolism* **155**, 155834 (2024).
21. Sasaki, H., Ohtsu, T., Ikeda, Y., Tsubosaka, M. & Shibata, S. Combination of meal and exercise timing with a high-fat diet influences energy expenditure and obesity in mice. *Chronobiol. Int.* **31**, 959–975 (2014).
22. Haxhi, J., Scotto di Palumbo, A. & Sacchetti, M. Exercising for metabolic control: is timing important?. *Ann. Nutr. Metab.* **62**, 14–25 (2013).
23. Teo, S. Y. M. et al. Exercise timing in type 2 diabetes mellitus: a systematic review. *Med. Sci. Sports Exerc.* **50**, 2387–2397 (2018).
24. Gabriel, B. M. & Zierath, J. R. Circadian rhythms and exercise - resetting the clock in metabolic disease. *Nat. Rev. Endocrinol.* **15**, 197–206 (2019).
25. Knaier, R. et al. Diurnal variation in maximum endurance and maximum strength performance: a systematic review and meta-analysis. *Med. Sci. Sports Exerc.* **54**, 169–180 (2022).
26. Hobson, R. M., Clapp, E. L., Watson, P. & Maughan, R. J. Exercise capacity in the heat is greater in the morning than in the evening in man. *Med. Sci. Sports Exerc.* **41**, 174–180 (2009).
27. Ammar, A., Chtourou, H. & Souissi, N. Effect of time-of-day on biochemical markers in response to physical exercise. *J. Strength Cond. Res.* **31**, 272–282 (2017).
28. Muoio, D. M. Metabolic inflexibility: when mitochondrial indecision leads to metabolic gridlock. *Cell* **159**, 1253–1262 (2014).
29. Goodpaster, B. H. & Sparks, L. M. Metabolic flexibility in health and disease. *Cell Metab.* **25**, 1027–1036 (2017).
30. Harfmann, B. D., Schroder, E. A. & Esser, K. A. Circadian rhythms, the molecular clock, and skeletal muscle. *J. Biol. Rhythms* **30**, 84–94 (2015).
31. Mayeuf-Louchart, A., Staels, B. & Duez, H. Skeletal muscle functions around the clock. *Diabetes Obes. Metab.* **17**, 39–46 (2015).
32. Schiaffino, S., Blaauw, B. & Dyar, K. A. The functional significance of the skeletal muscle clock: lessons from Bmal1 knockout models. *Skelet. Muscle* **6**, 33 (2016).
33. Bass, J. & Takahashi, J. S. Circadian integration of metabolism and energetics. *Science* **330**, 1349–1354 (2010).

34. Peek, C. B. et al. Circadian clock interaction with HIF1α mediates oxygenic metabolism and anaerobic glycolysis in skeletal muscle. *Cell Metab.* **25**, 86–92 (2017).

35. Basse, A. L. et al. Skeletal muscle insulin sensitivity show circadian rhythmicity which is independent of exercise training status. *Front. Physiol.* **9**, 1198 (2018).

36. Zhang, R., Lahens, N. F., Ballance, H. I., Hughes, M. E. & Hogenesch, J. B. A circadian gene expression atlas in mammals: implications for biology and medicine. *Proc. Natl. Acad. Sci. Usa.* **111**, 16219–16224 (2014).

37. Takahashi, J. S. Transcriptional architecture of the mammalian circadian clock. *Nat. Rev. Genet.* **18**, 164–179 (2017).

38. Woldt, E. et al. Rev-erb-α modulates skeletal muscle oxidative capacity by regulating mitochondrial biogenesis and autophagy. *Nat. Med.* **19**, 1039–1046 (2013).

39. Mayeuf-Louchart, A. et al. Rev-erb-α regulates atrophy-related genes to control skeletal muscle mass. *Sci. Rep.* **7**, 14383 (2017).

40. Amador, A. et al. Distinct roles for REV-ERBα and REV-ERBβ in oxidative capacity and mitochondrial biogenesis in skeletal muscle. *PloS One* **13**, e0196787 (2018).

41. Everett, L. J. & Lazar, M. A. Nuclear receptor rev-erbα: up, down, and all around. *Trends Endocrinol. Metab. TEM* **25**, 586–592 (2014).

42. Kojetin, D. J. & Burris, T. P. REV-ERB and ROR nuclear receptors as drug targets. *Nat. Rev. Drug Discov.* **13**, 197–216 (2014).

43. Gloston, G. F., Yoo, S.-H. & Chen, Z. J. Clock-enhancing small molecules and potential applications in chronic diseases and aging. *Front. Neurol.* **8**, 100 (2017).

44. Solt, L. A. et al. Regulation of circadian behaviour and metabolism by synthetic REV-ERB agonists. *Nature* **485**, 62–68 (2012).

45. Geldof, L., Deventer, K., Roels, K., Tudela, E. & Van Eeno, P. In vitro metabolic studies of REV-ERB agonists SR9009 and SR9011. *Int. J. Mol. Sci.* **17**, 1076 (2016).

46. Alibhai, F. J. et al. Disrupting the key circadian regulator CLOCK leads to age-dependent cardiovascular disease. *J. Mol. Cell. Cardiol.* **105**, 24–37 (2017).

47. Zhang, L. et al. REV-ERBα ameliorates heart failure through transcription repression. *JCI Insight* **2**, 95177 (2017).

48. Stujanna, E. N. et al. Rev-erb agonist improves adverse cardiac remodeling and survival in myocardial infarction through an anti-inflammatory mechanism. *PloS One* **12**, e0189330 (2017).

49. Montaigne, D. et al. Daytime variation of perioperative myocardial injury in cardiac surgery and its prevention by Rev-Erbα antagonism: a single-centre propensity-matched cohort study and a randomised study. *Lancet Lond. Engl.* **391**, 59–69 (2018).

50. Dierickx, P. et al. SR9009 has REV-ERB-independent effects on cell proliferation and metabolism. *Proc. Natl Acad. Sci. Usa.* **116**, 12147–12152 (2019).

51. Hill, D. W., Cureton, K. J. & Collins, M. A. Circadian specificity in exercise training. *Ergonomics* **32**, 79–92 (1989).

52. Hill, D. W., Leiferman, J. A., Lynch, N. A., Dangelmaier, B. S. & Burt, S. E. Temporal specificity in adaptations to high-intensity exercise training. *Med. Sci. Sports Exerc.* **30**, 450–455 (1998).

53. Bonetto, A., Andersson, D. C. & Waning, D. L. Assessment of muscle mass and strength in mice. *BoneKEy Rep.* **4**, 732 (2015).

54. Hong, S. et al. Dissociation of muscle insulin sensitivity from exercise endurance in mice by HDAC3 depletion. *Nat. Med.* **23**, 223–234 (2017).

55. Cho, H. et al. Regulation of circadian behaviour and metabolism by REV-ERB-α and REV-ERB-β. *Nature* **485**, 123–127 (2012).

56. Bothe, G. W., Haspel, J. A., Smith, C. L., Wiener, H. H. & Burden, S. J. Selective expression of Cre recombinase in skeletal muscle fibers. *Genes. N. Y. N. 2000* **26**, 165–166 (2000).

57. Iyer, S. R., Valencia, A. P., Hernández-Ochoa, E. O. & Lovering, R. M. In vivo assessment of muscle contractility in animal studies. *Methods Mol. Biol. Clifton NJ* **1460**, 293–307 (2016).

58. Brightwell, C. R. et al. In vivo measurement of knee extensor muscle function in mice. *J. Vis. Exp.* **10**, 3791/62211 (2021).

59. Michelucci, A. et al. Constitutive assembly of Ca2+ entry units in soleus muscle from calsequestrin knockout mice. *J. Gen. Physiol.* **154**, e202213114 (2022).

60. Song, S. et al. The HDAC3 enzymatic activity regulates skeletal muscle fuel metabolism. *J. Mol. Cell Biol.* **11**, 133–143 (2018).

61. Dyar, K. A. et al. Muscle insulin sensitivity and glucose metabolism are controlled by the intrinsic muscle clock. *Mol. Metab.* **3**, 29–41 (2014).

62. Guillaumond, F., Dardente, H., Giguère, V. & Cermakian, N. Differential control of Bmal1 circadian transcription by REV-ERB and ROR nuclear receptors. *J. Biol. Rhythms* **20**, 391–403 (2005).

63. Harding, H. P. & Lazar, M. A. The orphan receptor Rev-ErbA alpha activates transcription via a novel response element. *Mol. Cell. Biol.* **13**, 3113–3121 (1993).

64. Harding, H. P. & Lazar, M. A. The monomer-binding orphan receptor Rev-Erb represses transcription as a dimer on a novel direct repeat. *Mol. Cell. Biol.* **15**, 4791–4802 (1995).

65. Song, S. et al. The HDAC3 enzymatic activity regulates skeletal muscle fuel metabolism. *J. Mol. Cell Biol.* **11**, 133–143 (2018).

66. Ji, L. L., Kang, C. & Zhang, Y. Exercise-induced hormesis and skeletal muscle health. *Free Radic. Biol. Med.* **98**, 113–122 (2016).

67. Li, X., Yang, T. & Sun, Z. Hormesis in Health and Chronic Diseases. *Trends Endocrinol. Metab. TEM* **30**, 944–958 (2019).

68. Dalbram, E., Basse, A. L., Zierath, J. R. & Treebak, J. T. Voluntary wheel running in the late dark phase ameliorates diet-induced obesity in mice without altering insulin action. *J. Appl. Physiol. Bethesda Md. 1985* **126**, 993–1005 (2019).

69. Hesketh, S. J., Sexton, C. L., Wolff, C. A., Viggars, M. R. & Esser, K. A. Early morning run-training results in enhanced endurance performance adaptations in mice. *BioRxiv* https://doi.org/10.1101/2023.09.18.557933 (2023).

70. McArdle, W. D., Katch, F. I. & Katch, V. L. *Essentials of Exercise Physiology*, Vol. 753 (Lippincott Williams & Wilkins, 2006).

71. Dyar, K. A. et al. Transcriptional programming of lipid and amino acid metabolism by the skeletal muscle circadian clock. *PLoS Biol.* **16**, e2005886 (2018).

72. Hodge, B. A. et al. The endogenous molecular clock orchestrates the temporal separation of substrate metabolism in skeletal muscle. *Skelet. Muscle* **5**, 17 (2015).

73. Wada, T. et al. Deletion of Bmal1 prevents diet-induced ectopic fat accumulation by controlling oxidative capacity in the skeletal muscle. *Int. J. Mol. Sci.* **19**, 2813 (2018).

74. Harfmann, B. D. et al. Muscle-specific loss of Bmal1 leads to disrupted tissue glucose metabolism and systemic glucose homeostasis. *Skelet. Muscle* **6**, 12 (2016).

75. Yin, L. & Lazar, M. A. The orphan nuclear receptor Rev-erbalpha recruits the N-CoR/histone deacetylase 3 corepressor to regulate the circadian Bmal1 gene. *Mol. Endocrinol. Baltim. Md.* **19**, 1452–1459 (2005).

76. Yamamoto, H. et al. NCoR1 is a conserved physiological modulator of muscle mass and oxidative function. *Cell* **147**, 827–839 (2011).

77. Adamovich, Y. et al. Clock proteins and training modify exercise capacity in a daytime-dependent manner. *Proc. Natl Acad. Sci. Usa.* **118**, e2101115118 (2021).

78. Ramakrishnan, S. N., Lau, P., Burke, L. J. & Muscat, G. E. O. Rev-erbbeta regulates the expression of genes involved in lipid absorption in skeletal muscle cells: evidence for cross-talk between orphan nuclear receptors and myokines. *J. Biol. Chem.* **280**, 8651–8659 (2005).

79. Kim, H.-K., Radak, Z., Takahashi, M., Inami, T. & Shibata, S. Chrono-exercise: time-of-day-dependent physiological responses to exercise. *Sports Med. Health Sci.* **5**, 50–58 (2023).

80. Zhang, Y. et al. GENE REGULATION. Discrete functions of nuclear receptor Rev-erbα couple metabolism to the clock. *Science* **348**, 1488–1492 (2015).

81. Kang, M. J. et al. Metformin induces muscle atrophy by transcriptional regulation of myostatin via HDAC6 and FoxO3a. *J. Cachexia Sarcopenia Muscle* **13**, 605–620 (2022).

82. Augusto, V., Padovani, C. & Campos, G. E. R. Skeletal muscle fiber types in C57BL6J mice. *J. Morphol.* **54**, 45–56 (1976).

83. Song, S. et al. Myocardial Rev-erb-mediated diurnal metabolic rhythm and obesity paradox. *Circulation* **145**, 448–464 (2022).

Acknowledgements

Author contributions

J.L. characterized the baseline phenotype of KO mice and performed multi-omics data analysis. F.X. performed chronic exercise training and identified the time-dependent effects of exercise. A.C. performed additional muscle physiology and biochemistry analysis for chronic training and independently verified the time-dependent effects of exercise. U.K.S. and Y.W. assisted with bioinformatics analysis. S.H. conducted the initial mouse crossing. T.Y. performed ChIP-seq. J.L., F.X., A.C., and H.G.O. maintained the mouse colony. E.L. and T.S.K. performed ex vivo muscle physiology analysis. P.S. performed body composition and indirect calorimetry analyses. F.X. analyzed the data of indirect calorimetry with the assistance of ESO. J.L., F.X., A.C., U.K.S., Y.W., S.H., E.S.O., Y.S., E.L., T.S.K., X.H., and Z.S. analyzed and interpreted data. L.C. provided financial support for J.L. L.C., X.H., and Z.S. obtained funding. Z.S. conceived and designed the study. JL, F.X., A.C., and Z.S. wrote the manuscript with the help of other authors.

Competing interests

The authors declare no competing interests.

Additional information

Supplementary information The online version contains supplementary material available at https://doi.org/10.1038/s41467-025-60520-y.

Correspondence and requests for materials should be addressed to Xinguo Hou or Zheng Sun.

Peer review information *Nature Communications* thanks Joseph Baur, and the other, anonymous, reviewers for their contribution to the peer review of this work. A peer review file is available.

Reprints and permissions information is available at http://www.nature.com/reprints

Publisher's note Springer Nature remains neutral with regard to jurisdictional claims in published maps and institutional affiliations.